AD-783 276

THEORETICAL STUDY OF NON-STANDARD
IMAGING CONCEPTS

David L. Fried

Optical Science Consultants

Prepared for:

Rome Air Development Center
Advanced Research Projects Agency

May 1974

REPORT DOCUMENTATION PAGE		READ INSTRUCTIONS BEFORE COMPLETING FORM
1. REPORT NUMBER RADC-TR-74-185	2. GOVT ACCESSION NO.	3. RECIPIENT'S CATALOG NUMBER AD 783 276
4. TITLE *(and Subtitle)* Theoretical Study of Non-Standard Imaging Concepts		5. TYPE OF REPORT & PERIOD COVERED Interim Technical Report 15 Jan 74 – 15 May 74
		6. PERFORMING ORG. REPORT NUMBER
7. AUTHOR(s) David L. Fried		8. CONTRACT OR GRANT NUMBER(s) F30602-74-C-0115
9. PERFORMING ORGANIZATION NAME AND ADDRESS Optical Science Consultants P O Box 388 Yorba Linda CA 92686		10. PROGRAM ELEMENT, PROJECT, TASK AREA & WORK UNIT NUMBERS 62301E 26460102
11. CONTROLLING OFFICE NAME AND ADDRESS Defense Advanced Research Projects Agency 1400 Wilson Blvd Arlington VA 22209		12. REPORT DATE May 1974
		13. NUMBER OF PAGES 71
14. MONITORING AGENCY NAME & ADDRESS*(if different from Controlling Office)* Rome Air Development Center (OCSE) ATTN: Capt Darryl P. Greenwood Griffiss AFB NY 13441		15. SECURITY CLASS. *(of this report)* UNCLASSIFIED
		15a. DECLASSIFICATION/DOWNGRADING SCHEDULE

16. DISTRIBUTION STATEMENT *(of this Report)*

Approved for public release; distribution unlimited.

Reproduced from best available copy.

17. DISTRIBUTION STATEMENT *(of the abstract entered in Block 20, if different from Report)*

Approved for public release; distribution unlimited.

18. SUPPLEMENTARY NOTES

None

19. KEY WORDS *(Continue on reverse side if necessary and identify by block number)*

Imaging
Atmospheric Optics
Propagation
Turbulence

20. ABSTRACT *(Continue on reverse side if necessary and identify by block number)*

This report presents the more significant and complete results to date on a program of theoretical study related to unconventional imagery and techniques for suppression of atmospheric turbulence effects on image quality. The objective of this work has been to develop an understanding and quantitative theory of those aspects of propagation through atmospheric turbulence that would limit the performance of unconventional imagery techniques, and to develop a basis for quantifying the effective magnitude of atmospheric turbulence.

DD FORM 1473 EDITION OF 1 NOV 65 IS OBSOLETE
1 JAN 73

UNCLASSIFIED

15

Continued

In this report, we present results of an analysis of the isoplanatic aspects of predetection compensation imagery. We have developed formal theoretical results for how the achievable modulation transfer function for predetection compensation varies with the angular size of the image, or with the angular separation between the image and the reference source. Detailed evaluation is carried out for propagation over a path with uniform optical strength of turbulence along the path (nominally a horizontal path). It is found that for propagation along a horizontal path of length z, if the wavelength and strength of turbulence are such as to result in a coherence length r_o, then the angular separation between the image and the reference must be less than $\vartheta_o = r_o/2z$ if predetection compensation is to produce useful imagery of fine details.

In order to extend the calculations of the isoplanatic aspects of predetection compensation to include results for ground-based viewing of space objects, it is necessary to have a model for the vertical distribution of the optical strength of turbulence. We have generated such a model, making use of the low altitude aircraft thermal probe measurements of Koprov and Tsvang, and the high altitude balloon thermal probe data of Bufton. The model is presented in terms of a table of numerical values, along with a discussion of the data processing details by which the model was extracted from the available raw data.

As part of the problem of measuring the optical effects of turbulence over finite non-horizontal propagation paths, such as between an aircraft and the ground, this report considers the possibility of using differential angle of arrival measurements. The advantage of this type of measurement is that it allows tracking of a point source and measures wavefront distortion in terms of (differential) angle of arrival at two sub-apertures on the same mount, giving meaningful results without placing significant constraint on the tracking accuracy of the mount. Significantly, the basic equipment for this type of measurement is available at RADC. The questions to be answered by theoretical analysis are how does the mean square differential angle of arrival vary with separation of the two subapertures, and is the expected value for the largest achievable separation great enough compared to equipment measurement precision to allow for meaningful measurements. These questions are answered in this report. The dependence is evaluated and tables of results are presented. It is found that measurement accuracies are adequate to allow for propagation path characterization with modest (i.e., 5% to 10%) precision.

1a

THEORETICAL STUDY OF NON-STANDARD IMAGING CONCEPTS

David L. Fried

ib

This report has been reviewed by the RADC Information Office (OI), and is releasable to the National Technical Information Service (NTIS).

This technical report has been reviewed and is approved.

Darryl P. Greenwood
RADC Project Engineer

If this copy is not needed, return to RADC (OCSE) Darryl P. Greenwood, GAFB, NY 13441.

ii

Summary

This report presents the more significant and complete results to date on a program of theoretical study related to unconventional imagery and techniques for suppression of atmospheric turbulence effects on image quality. The objective of this work has been to develop an understanding and quantitative theory of those aspects of propagation through atmospheric turbulence that would limit the performance of unconventional imagery techniques, and to develop a basis for quantifying the effective magnitude of atmospheric turbulence.

In this report, we present results of an analysis of the isoplanatic aspects of predetection compensation imagery. We have developed formal theoretical results for how the achievable modulation transfer function for predetection compensation varies with the angular size of the image, or with the angular separation between the image and the reference source. Detailed evaluation is carried out for propagation over a path with uniform optical strength of turbulence along the path (nominally a horizontal path). It is found that for propagation along a horizontal path of length z , if the wavelength and strength of turbulence are such as to result in a coherence length r_0 , then the angular separation between the image and the reference must be less than $\vartheta_0 = r_0/2z$ if predetection compensation is to produce useful imagery of fine details.

In order to extend the calculations of the isoplanatic aspects of predetection compensation to include results for ground-based viewing of space objects, it is necessary to have a model for the vertical distribution of the optical strength of turbulence. We have generated such a model, making use of the low altitude aircraft thermal probe measurements of Koprov and Tsvang, and the high altitude balloon thermal probe data of

Bufton. The model is presented in terms of a table of numerical values, along with a discussion of the data processing details by which the model was extracted from the available raw data.

As part of the problem of measuring the optical effects of turbulence over finite non-horizontal propagation paths, such as between an aircraft and the ground, this report considers the possibility of using differential angle of arrival measurements. The advantage of this type of measurement is that it allows tracking of a point source and measures wavefront distortion in terms of (differential) angle of arrival at two sub-apertures on the same mount, giving meaningful results without placing significant constraint on the tracking accuracy of the mount. Significantly, the basic equipment for this type of measurement is available at RADC. The questions to be answered by theoretical analysis are how does the mean square differential angle of arrival vary with separation of the two subapertures, and is the expected value for the largest achievable separation great enough compared to equipment measurement precision to allow for meaningful measurements. These questions are answered in this report. The dependence is evaluated and tables of results are presented. It is found that measurement accuracies are adequate to allow propagation path characterization with modest (i.e., 5% to 10%) precision.

TABLE OF CONTENTS

TABLE LIST

FIGURE LIST

ABSTRACT

In Chapter I, the concept of predetection compensation imagery is defined and a formal analysis of the effects of atmospheric turbulence on the compensated image MTF is set up. An expression is obtained for the MTF in terms of an integral over the propagation path. The integrand is a function of the refractive-index structure constant, the image frequency, f, the angular separation between the target object and the reference source, ϑ, and the angle, ϕ, between the vector aspects of f and ϑ. For horizontal propagation, it is found that two parameters can be defined which govern the quality of the compensated MTF. These are ϑ_0, the predetection compensation critical angle, and f_0, the transition frequency. We find that for image frequencies below f_0, there is no useful compensation, in fact we suffer an effective doubling of the strength of the turbulence. (However, if f_0 is small enough, this is of no consequence.) For image frequencies greater than f_0, the MTF is down from diffraction-limited by no more than a factor of $\exp[-2.58\,(\vartheta/\vartheta_0)^{5/3}]$. So long as ϑ is made less than ϑ_0, the compensation will be quite effective. Expressions obtained for ϑ_0 and f_0 are $\vartheta_0 = r_0/2z$ and $f_0 = 2\vartheta z/\lambda$, where z is the path length and r_0 is the critical coherence length for conventional long exposure imagery.

In Chapter II, medium and high altitude thermal probe data by Bufton, and low altitude thermal probe data by Koprov and Tsvang are processed to provide a smooth distribution for the refractive-index structure constant in the atmosphere. The model is used to calculate the critical length for diffraction-limited imaging, i.e., r_0, and the log-amplitude variance, i.e., σ_ℓ^2. Comparison with measured values shows very good agreement for r_0, and only fair agreement for σ_ℓ^2.

In Chapter III, the problem of measuring differential angle of arrival through two relatively small apertures of variable separation is considered. The motivation is to evaluate the practicality of a measurement program using such a quantity to observe atmospheric turbulence wavefront distortion effects when one end of the link is moving and can not be tracked precisely. Theoretical results for the mean square difference in angle of arrival are developed. Numerical results have been calculated using a computer. Comparison of expected magnitude of effects with available measurement instrument precision indicates that the experiment should be possible, but will depend on our ability to achieve an rms single axis angle of arrival measurement precision of the order of 0.1 arc seconds or better.

CHAPTER I

Isoplanatic Aspects

of

Predetection Compensation Imagery

Introduction

The concept of isoplanatism refers to the fact that over some size field-of-view the image of an object will suffer the same degradation from diffraction-limited quality, independent of where the object is within that field-of-view. It is common usage to refer to the field-of-view as the isoplanatic patch. As thus defined, the concept of isoplanatism refers basically to the performance of a lens or mirror imaging system. However, this same concept can be applied in discussing the effect of atmospheric turbulence on an otherwise ideal imaging system. It is in this context that we shall consider the subject of isoplanatism.

Before proceeding farther, we wish to make certain disclaimers and place certain bounds on the extent of the problem we shall be treating. First of all, we call attention to the fact that it is by no means clear, or even likely that atmospheric turbulence induced resolution effects will be strictly constant over any non-trivial size field-of-view. Rather, it is likely that whatever resolution variation there is over the field-of-view will show a monotonic dependence on the size of the field angle. We could define the isoplanatic patch as being determined by the size of the field angle that makes the variation just reach some (arbitrarily chosen) level of significance. However, rather than engage in a matter of such arbitrary nature, we shall simply seek knowledge of the field-angle dependence, which we shall refer to as the isoplanatic dependence of resolution, and avoid, as much as possible, discussion of the size of the isoplanatic patch.

Secondly, we wish to take note of the fact that there are a variety of distinct conventional and unconventional imaging techniques presently being considered for imaging through atmospheric turbulence. Each of these techniques functions in a different manner and is sensitive to somewhat different aspects of the optical effects of atmospheric turbulence. There is, therefore, no reason to believe that the isoplanatic dependence of any two of these techniques will be the same. In this paper, we shall be considering

- 2 -

one of the more interesting of the unconventional imaging techniques, which we refer to as predetection compensation. There is no assurance that the isoplanatism dependence that we shall develop in this paper for predetection compensation imaging will be applicable to any other imaging technique, and we caution the reader against assuming that this result necessarily is relevant to any of these other techniques. (At a later time, we hope to extend our work to cover some of these other techniques.)

Predetection Compensation

Predetection compensation is the generic term used to describe any one of a number of techniques that seek to estimate, in real time, the nature of the atmospheric turbulence induced wavefront distortion at the imaging system's collection aperture, and in real time compensate for the wavefront distortion. In this way, the image as formed is compensated for turbulence effects. (The term "predetection compensation" is perhaps best understood in juxtaposition to the term "postdetection compensation." Postdetection compensation is the process of correcting the distorted image after it is formed, by some form of modulation transfer function compensation, or by some more or less equivalent technique.)

The key to predetection compensation lies in two areas. The first of these is the ability to in real time estimate the nature of the phase distortion and perhaps also the intensity variation at the aperture. The second key is the ability, in real time, to modify the optical system so as to correct for the phase, and possibly also the intensity variations, so that the corrected optical signal contains only the information descriptive of the object being viewed. Techniques are under development by several organizations aimed at demonstrating both of these capabilities and producing a predetection compensated image.

It would be beside the point to go into the details of the techniques that are being considered. Our concern here is with the evaluation of one

potential limitation in the predetection compensation concept. This limitation relates to the isoplanatic aspect of the process. We are concerned with the fact that in order to estimate the phase and intensity variations, all techniques that have been proposed require the observation of a reference source. The estimated variation is then used to correct the wave coming from some point on the object of interest. In general, the field angle associated with the reference source will not be identical to the field angle for the point on the object we are imaging. Our concern is to develop a quantitative understanding of how the angular separation between the reference source and the point being imaged affects the resolution of the compensated image. We consider this to be the problem of isoplanatism for predetection compensated imagery.

Analytic Problem Definition

For the purposes of analysis, we shall consider the problem of predetection compensated imaging of a point target source at field angle $\vec{\theta}_1$, using a point reference source at field angle $\vec{\theta}_2$. We shall study the ensemble average modulation transfer function for the predetection compensated target image, $\langle \tau_{PDC}(\vec{f}) \rangle$, at image frequency $\vec{f}$ (in cycles per radian field-of-view), as a function of the angular separation

$$\vec{\vartheta} = \vec{\theta}_1 - \vec{\theta}_2 \qquad . \tag{1}$$

In many propagation situations, intensity variations are minor, i.e., the log-amplitude variation is much less than one neper, and so there is no great utility in correcting for intensity variations. Only phase variation correction would be of concern. In other propagation situations, however, intensity variations could be sizable, and it would be necessary to utilize intensity compensation in order to obtain a well compensated image. While such compensation is somewhat more difficult than phase compensation, there is nothing fundamental that prevents such compensation from being utilized. In all cases, the use of intensity compensation

- 4 -

along with phase compensation will give at least as good, if not a significantly better compensated image than would the use of phase compensation alone. Consequently, to investigate the $\vec{\vartheta}$-dependence of the predetection compensated image, we shall treat the case in which both phase and intensity variations are corrected.

We shall use the notation $\ell(\vec{x}, \vec{\theta}_1)$ and $\phi(\vec{x}, \vec{\theta}_1)$ to denote the instantaneous turbulence induced variation of log-amplitude and phase, respectively, at a point $\vec{x}$ on the collection aperture plane, for a wave coming from the point target source at $\vec{\theta}_1$. Similarly, we shall use $\ell(\vec{x}, \vec{\theta}_2)$ and $\phi(\vec{x}, \vec{\theta}_2)$ to denote the same quantities for the wave coming from the point reference source at $\vec{\theta}_2$. In predetection compensation, we form estimates of $\ell(\vec{x}, \vec{\theta}_2)$ and $\phi(\vec{x}, \vec{\theta}_2)$, which we shall assume for the purpose of this analysis are perfect estimates, and correct the received wave from the target accordingly. This means that we form our image using a wave with residual log-amplitude and phase errors at $\vec{x}$, given by

$$\Delta\ell(\vec{x}, \vec{\vartheta}) = \ell(\vec{x}, \vec{\theta}_1) - \ell(\vec{x}, \vec{\theta}_2) \quad , \tag{2a}$$

$$\Delta\phi(\vec{x}, \vec{\vartheta}) = \phi(\vec{x}, \vec{\theta}_1) - \phi(\vec{x}, \vec{\theta}_2) \quad , \tag{2b}$$

respectively. If there were no field angle dependence, so that $\ell(\vec{x}, \vec{\theta}_1)$ exactly equaled $\ell(\vec{x}, \vec{\theta}_2)$ and $\phi(\vec{x}, \vec{\theta}_1)$ exactly equaled $\phi(\vec{x}, \vec{\theta}_2)$, then the residual errors would be zero and the predetection compensated image would be ideal. However, to the extent that isoplanatism is less than perfect, the residual errors will be non-zero and the predetection compensated image will be less than ideal.

The calculation of the modulation transfer function now proceeds in almost exactly the same manner we have utilized previously[1] for calculation of the long exposure MTF for conventional imagery. If we let $U(\vec{x})$ denote the scalar form of the compensated electromagnetic field at aperture position $\vec{x}$, and let $u(\vec{y})$ denote the associated image scalar form of the

electromagnetic field at the position $\vec{y}$ in the focal plane, then it is well known that

$$u(\vec{y}) = A \int d\vec{x}\, U(\vec{x}) \exp(-ik\vec{x} \cdot \vec{y}) \qquad , \qquad (3)$$

where A is a constant of proportionality and $k = 2\pi/\lambda$ is the optical wave number. (Here and throughout this paper integrals without explicitly stated limits are to be understood as being definite integrals with infinite limits. In Eq. (3), the effective limits of the integration are provided by the fact that $U(\vec{x})$ vanishes for $\vec{x}$ outside the limits of the collection aperture.) The instantaneous power distribution in the focal plane is proportional to $|u(\vec{y})|^2$. Since the MTF is just the fourier transform of the impulse response, which $|u(\vec{x})|^2$ represents, we can write for the MTF at image frequency $\vec{f}$

$$\tau_{PDC}(\vec{f}) = B \int d\vec{y}\, |u(\vec{y})|^2 \exp(2\pi i\vec{f} \cdot \vec{y}) \qquad , \qquad (4)$$

where B is a normalization constant chosen to make $\tau_{PDC}(0) = 1$.

If we combine Eq.'s (3) and (4), we get

$$\tau_{PDC}(\vec{f}) = A^2 B \iiint d\vec{y}\, d\vec{x}\, d\vec{x}'\, U^*(\vec{x}')\, U(\vec{x}) \exp\left[2\pi i\vec{y} \cdot \left(\vec{f} + \frac{\vec{x}'}{\lambda} - \frac{\vec{x}}{\lambda}\right)\right] . \quad (5a)$$

Noting that carrying out the $\vec{y}$-integration gives rise to a delta function which then allows the $\vec{x}'$-integration trivially, we get

$$\tau_{PDC}(\vec{f}) = A^2 B \int d\vec{x}\, U^*(\vec{x} - \lambda\vec{f})\, U(\vec{x}) \qquad . \qquad (5b)$$

Now introducing $W(\vec{x})$ to define a circular aperture of diameter D, according to the equation

$$W(\vec{x}) = \begin{cases} 1 , & \text{if} \quad |\vec{x}| \leq \frac{1}{2} D \\ 0 , & \text{if} \quad |\vec{x}| > \frac{1}{2} D \end{cases} , \qquad (6)$$

we can write the compensated scalar field at the aperture, $U(\vec{x})$ in terms of the compensated log-amplitude and phase errors $\Delta\ell(\vec{x},\vec{\vartheta})$ and $\Delta\phi(\vec{x},\vec{\vartheta})$, respectively. We have

$$U(\vec{x}) = W(\vec{x}) \exp\left[\Delta\ell(\vec{x},\vec{\vartheta}) + i\,\Delta\phi(\vec{x},\vec{\vartheta})\right] \quad , \tag{7}$$

and if we substitute this into Eq. (5b), we get

$$\tau_{PDC}(\vec{f}) = A^2 B \int d\vec{x}\, W(\vec{x} - \lambda\vec{f})\, W(\vec{x}) \exp\left\{\left[\Delta\ell(\vec{x},\vec{\vartheta}) + \Delta\ell(\vec{x}-\lambda\vec{f},\vec{\vartheta})\right] \right. $$
$$\left. + i\left[\Delta\phi(\vec{x}) - \Delta\phi(\vec{x}-\lambda\vec{f},\vec{\vartheta})\right]\right\} \quad . \tag{8}$$

The ensemble average predetection compensated modulation transfer function can now be written as

$$\langle\tau_{PDC}(\vec{f})\rangle = A^2 B \int d\vec{x}\, W(\vec{x}-\lambda\vec{f})\, W(\vec{x})\, \langle\exp\left\{\left[\Delta\ell(\vec{x},\vec{\vartheta}) + \Delta\ell(\vec{x}-\lambda\vec{f},\vec{\vartheta})\right]\right. $$
$$\left. + i\left[\Delta\phi(\vec{x},\vec{\vartheta}) - \Delta\phi(\vec{x}-\lambda\vec{f},\vec{\vartheta})\right]\right\}\rangle \quad . \tag{9a}$$

Since the wavefront distortion statistics are homogeneous so that the ensemble average on the right hand side of Eq. (9a) is not actually a function of $\vec{x}$, we can write

$$\langle\tau_{PDC}(\vec{f})\rangle = \tau_{DL}(f)\, M(\lambda\vec{f},\vec{\vartheta}) \quad , \tag{9b}$$

where $\tau_{DL}(f)$ is given by the expression

$$\tau_{DL}(f) = A^2 B \int d\vec{x}\, W(\vec{x}-\lambda\vec{f})\, W(\vec{x}) \quad , \tag{10}$$

and is, as we shall see, the MTF of a diffraction-limited circular aperture of diameter D . $M(\lambda\vec{f},\vec{\vartheta})$ is given by the expression

$$M(\lambda \vec{f}, \vec{\vartheta}) = \langle \exp \{[\Delta \ell(\vec{x}, \vec{\vartheta}) + \Delta \ell(\vec{x} - \lambda \vec{f}, \vec{\vartheta})] + i[\Delta \phi(\vec{x}, \vec{\vartheta}) - \Delta \phi(\vec{x} - \lambda \vec{f}, \vec{\vartheta})]\} \rangle . \quad (11)$$

The integral on the right hand side of Eq. (10) can be recognized as the area of overlap of two circles of diameter D whose centers are displaced a distance λf . Making use of a little trigonometry, it is easy to show that

$$\tau_{DL}(f) = \frac{2}{\pi} \left\{ \cos^{-1}\left(\frac{\lambda f}{D}\right) - \left(\frac{\lambda f}{D}\right)\left[1 - \left(\frac{\lambda f}{D}\right)^2\right]^{\frac{1}{2}} \right\} , \quad (12)$$

where we have anticipated the fact that $M(0, \vartheta)$ is equal to unity and adjusted the normalization constant B so that the MTF will have unity value at $f = 0$. We recognize $\tau_{DL}(f)$ in Eq. (12) as being the well known expression for the MTF of a diffraction-limited optical system with a circular aperture of diameter D .

Our problem at this point is reduced to evaluation of $M(\lambda \vec{f}, \vec{\vartheta})$. To the extent that this quantity equals unity, the predetection compensated modulation transfer function is ideal, and to the extent that it deviates from unity (we shall see that it is always less than or equal to unity), the predetection compensated modulation transfer function is less than ideal. The balance of the analysis in this paper is devoted to the evaluation of $M(\lambda \vec{f}, \vec{\vartheta})$. In the next section, we develop an expression for M in terms of quantities describing optical propagation statistics, and in the section after that, we treat the propagation problem to obtain a formulation of these statistics.

Representation for $M(\lambda \vec{f}, \vec{\vartheta})$

In order to reduce the right hand side of Eq. (11), we start by noting that if α and β are independent gaussian random variables, each with zero mean value, and if a and b are arbitrary constants, then it is easy to show that

- 8 -

$$\langle \exp (a\alpha + b\beta) \rangle = \exp \left[\tfrac{1}{2} (a^2 \langle \alpha^2 \rangle + b^2 \langle \beta^2 \rangle) \right] \quad . \tag{13}$$

Because the log-amplitude ℓ and the phase ϕ are themselves gaussian, it follows that the compensated log-amplitude error $\Delta\ell$ and the compensated phase error $\Delta\phi$ are each gaussian. It follows from consideration of Eq.'s (2a and b) and the fact that the propagation statistics are stationary in terms of the field angle dependence (in this case, $\vec{\theta}_1$ and $\vec{\theta}_2$) that $\Delta\ell$ and $\Delta\phi$ both have zero mean value. It can be shown, using the fact that the propagation statistics are isotropic, that the quantities $[\Delta\ell(\vec{x},\vec{\vartheta}) + \Delta\ell(\vec{x}-\lambda\vec{f},\vec{\vartheta})]$ and $[\Delta\phi(\vec{x},\vec{\vartheta}) - \Delta\phi(\vec{x}-\lambda\vec{f},\vec{\vartheta})]$ are independent. Obviously, then, Eq. (13) can be applied to the evaluation of the right hand side of Eq. (11). We get

$$M(\lambda\vec{f},\vec{\vartheta}) = \exp \left\{ \tfrac{1}{2} \langle [\Delta\ell(\vec{x},\vec{\vartheta}) + \Delta\ell(\vec{x}-\lambda\vec{f},\vec{\vartheta})]^2 \rangle \right.$$

$$\left. - \tfrac{1}{2} \langle [\Delta\phi(\vec{x},\vec{\vartheta}) - \Delta\phi(\vec{x}-\lambda\vec{f},\vec{\vartheta})]^2 \rangle \right\} \quad . \tag{14}$$

In order to reduce the terms in the exponent, we introduce the two structure function related statistical quantities

$$\mathcal{D}_\ell(\vec{\rho},\vec{\vartheta}) = \langle [\ell(\vec{x},\vec{\theta}_1) - \ell(\vec{x}',\vec{\theta}_1)][\ell(\vec{x},\vec{\theta}_2) - \ell(\vec{x}',\vec{\theta}_2)] \rangle \quad , \tag{15a}$$

and

$$\mathcal{D}_\phi(\vec{\rho},\vec{\vartheta}) = \langle [\phi(\vec{x},\vec{\theta}_1) - \phi(\vec{x}',\vec{\theta}_1)][\phi(\vec{x},\vec{\theta}_2) - \phi(\vec{x}',\vec{\theta}_2)] \rangle \quad , \tag{15b}$$

where

$$\vec{\rho} = \vec{x} - \vec{x}' \quad . \tag{16}$$

We shall refer to these two quantities as the log-amplitude and the phase hyperstructure functions. (In the limiting case of $\vec{\theta}_1 = \vec{\theta}_2$ so that $\vec{\vartheta} = 0$, the hyperstructure functions reduce to the ordinary structure functions.)

If we make use of Eq. (2b), we see that the phase dependence in Eq. (14) can be written as

$$\langle [\Delta\phi(\vec{x},\vec{\vartheta}) - \Delta\phi(\vec{x} - \lambda\vec{f},\vec{\vartheta})]^2 \rangle$$

$$= \langle \{[\phi(\vec{x},\vec{\theta}_1) - \phi(\vec{x},\vec{\theta}_2)] - [\phi(\vec{x}-\lambda\vec{f},\vec{\theta}_1) - \phi(\vec{x}-\lambda\vec{f},\vec{\theta}_2)]\}^2 \rangle$$

$$= \langle \{[\phi(\vec{x},\vec{\theta}_1) - \phi(\vec{x}-\lambda\vec{f},\vec{\theta}_1)] - [\phi(\vec{x},\vec{\theta}_2) - \phi(\vec{x}-\lambda\vec{f},\vec{\theta}_2)]\}^2 \rangle$$

$$= 2\,[\mathfrak{D}_\phi(\lambda\vec{f},0) - \mathfrak{D}_\phi(\lambda\vec{f},\vec{\vartheta})] \qquad . \tag{17}$$

Reduction of the log-amplitude dependence in Eq. (14) is somewhat more complex. It is most conveniently accomplished by introducing the log-amplitude hypercovariance function

$$\mathfrak{S}_\ell(\vec{\rho},\vec{\vartheta}) = \langle [\ell(\vec{x},\vec{\theta}_1) - \overline{\ell}][\ell(\vec{x'},\vec{\theta}_2) - \overline{\ell}] \rangle \qquad , \tag{18}$$

where

$$\overline{\ell} = \langle \ell(\vec{x},\vec{\theta}) \rangle \qquad . \tag{19}$$

It is easy to show that

$$\langle \{[\ell(\vec{x},\vec{\theta}_1) - \ell(\vec{x},\vec{\theta}_2)] \pm [\ell(\vec{x'},\vec{\theta}_1) - \ell(\vec{x'},\vec{\theta}_2)]\}^2 \rangle$$

$$= 4\,\{[\mathfrak{S}_\ell(0,0) - \mathfrak{S}_\ell(0,\vec{\vartheta})] \pm [\mathfrak{S}_\ell(\vec{\rho},0) - \tfrac{1}{2}\mathfrak{S}_\ell(\vec{\rho},\vec{\vartheta})$$

$$- \tfrac{1}{2}\mathfrak{S}_\ell(\vec{\rho},-\vec{\vartheta})]\} \qquad . \tag{20}$$

By making use of Eq. (20), we can write the log-amplitude dependence of the exponent in Eq. (14) as

$$\langle [\Delta\ell(\vec{x},\vec{\vartheta}) + \Delta\ell(\vec{x}-\lambda\vec{f},\vec{\vartheta})]^2 \rangle$$

$$= \langle \{[\ell(\vec{x},\vec{\theta}_1) - \ell(\vec{x},\vec{\theta}_2)] + [\ell(\vec{x}-\lambda\vec{f},\vec{\theta}_1) - \ell(\vec{x}-\lambda\vec{f},\vec{\theta}_2)]\}^2 \rangle$$

$$= -\left\langle \left\{ \left[\ell(\vec{x}, \vec{\theta}_1) - \ell(\vec{x}, \vec{\theta}_2) \right] - \left[\ell(\vec{x} - \lambda \vec{f}, \vec{\theta}_1) - \ell(\vec{x} - \lambda \vec{f}, \vec{\theta}_2) \right] \right\}^2 \right\rangle$$
$$+ 8 \left[\mathfrak{S}_\ell(0, 0) - \mathfrak{S}_\ell(0, \vec{\vartheta}) \right]$$

$$= -\left\langle \left\{ \left[\ell(\vec{x}, \vec{\theta}_1) - \ell(\vec{x} - \lambda \vec{f}, \vec{\theta}_1) \right] - \left[\ell(\vec{x}, \vec{\theta}_2) - \ell(\vec{x} - \lambda \vec{f}, \vec{\theta}_2) \right] \right\}^2 \right\rangle$$
$$+ 8 \left[\mathfrak{S}_\ell(0, 0) - \mathfrak{S}_\ell(0, \vec{\vartheta}) \right]$$

$$= - 2\left[\mathfrak{D}_\ell(\lambda \vec{f}, 0) - \mathfrak{D}_\ell(\lambda \vec{f}, \vec{\vartheta}) \right] + 8\left[\mathfrak{S}_\ell(0, 0) - \mathfrak{S}_\ell(0, \vec{\vartheta}) \right] \quad . \tag{21}$$

Now if we substitute Eq.'s (17) and (21) into Eq. (14), we get

$$M(\lambda \vec{f}, \vec{\vartheta}) = \exp \left\{ - \left[\mathfrak{D}_\ell(\lambda \vec{f}, 0) - \mathfrak{D}_\ell(\lambda \vec{f}, \vec{\vartheta}) \right] + 4 \left[\mathfrak{S}_\ell(0, 0) - \mathfrak{S}_\ell(0, \vec{\vartheta}) \right] \right.$$
$$\left. - \left[\mathfrak{D}_\phi(\lambda \vec{f}, 0) - \mathfrak{D}_\phi(\lambda \vec{f}, \vec{\vartheta}) \right] \right\}$$

$$\Rightarrow \exp \left\{ - \left[\mathfrak{D}_\ell(\lambda \vec{f}, 0) - \mathfrak{D}_\ell(\lambda \vec{f}, \vec{\vartheta}) \right] - \left[\mathfrak{D}_\phi(\lambda \vec{f}, 0) - \mathfrak{D}_\phi(\lambda \vec{f}, \vec{\vartheta}) \right] \right\} \ , \tag{22}$$

where we have dropped the $\mathfrak{S}_\ell(0, 0) - \mathfrak{S}_\ell(0, \vec{\vartheta})$ dependence in the exponent
since it does not represent an image frequency dependence. Its contribu-
tion is multiplicative and is absorbed into the normalization constant B
in going from Eq. (9a) to Eq. (9b). (As we shall see, dropping this
$\mathfrak{S}$-dependence insures that $M(\lambda \vec{f}, \vec{\vartheta})$ will have unity value for $\vec{f} = 0$.) Eq. (22)
represents the end point of this section -- a representation of $M(\lambda \vec{f}, \vec{\vartheta})$ in
terms of the propagation statistics. In the next section, we take up the prob-
lem of calculating these statistics.

Propagation Statistics

The problem of calculating the propagation statistics associated with
the hyperstructure functions has been treated previously.[2] The published
results can be written in the form

$$\mathfrak{D}_\ell(\vec{\rho}, \vec{\vartheta}) = \frac{8.16 \, k^2}{4 \pi^2} \int_0^z dv \, C_N^2 \int d\vec{\sigma} \left[1 - \exp(i \, \vec{\sigma} \cdot \vec{\rho}) \right] \sigma^{-11/3}$$
$$\times \left[\cos(2\vec{\sigma} \cdot \vec{\vartheta} v) - \cos(v \, \sigma^2 / k) \right] \ , \tag{23a}$$

- 11 -

$$\mathcal{D}_\phi(\vec{\rho},\vec{\vartheta}) = \frac{8.16\,k^2}{4\,\pi^2}\int_0^z dv\,C_N^2\,\int d\vec{\sigma}\,[\,1 - \exp(i\,\vec{\sigma}\cdot\vec{\rho})]\,\sigma^{-11/3}$$

$$\times\,[\cos(2\vec{\sigma}\cdot\vec{\vartheta}v) + \cos(v\,\sigma^2/k)]\quad. \tag{23h}$$

The $\vec{\sigma}$-integration is understood to be two-dimensional, in the plane perpendicular to the z-axis. (C_N^2 , of course, denotes the refractive-index structure constant, and $k = 2\pi/\lambda$ is the optical wave number.)

If we substitute these results into Eq. (22), we see that we can write

$$M(\lambda\vec{f},\vec{\vartheta}) = \exp[-\mathcal{m}(\lambda\vec{f},\vec{\vartheta})]\quad, \tag{24'}$$

where

$$\mathcal{m}(\lambda\vec{f},\vec{\vartheta}) = \frac{8.16\,k^2}{2\,\pi^2}\int_0^z dv\,C_N^2\,\int d\vec{\sigma}\,[\,1 - \exp(i\,\vec{\sigma}\cdot\lambda\vec{f})]\,\sigma^{-11/3}$$

$$\times\,[\,1 - \cos(2\vec{\sigma}\cdot\vec{\vartheta}v)]\quad. \tag{24}$$

Our problem at this point is the reduction of $\mathcal{m}(\lambda\vec{f},\vec{\vartheta})$ to numerical results. We take this up in the following sections.

Preliminary Reduction of $\mathcal{m}(\lambda\vec{f},\vec{\vartheta})$

Without having to make any assumptions as to the nature of the distribution of C_N^2 along the propagation path, we can carry out the $\vec{\sigma}$-integration. To do this, we first rewrite Eq. (24) in the form

$$\mathcal{m}(\lambda\vec{f},\vec{\vartheta}) = \frac{8.16\,k^2}{2\,\pi^2}\int_0^z dv\,C_N^2\,\int d\vec{\sigma}\,\sigma^{-11/3}\,\{1 - \exp(i\,\vec{\sigma}\cdot\lambda\vec{f})$$

$$-\tfrac{1}{2}\exp(2\,i\vec{\sigma}\cdot\vec{\vartheta}v) - \tfrac{1}{2}\exp(-2\,i\vec{\sigma}\cdot\vec{\vartheta}v)$$

$$+\tfrac{1}{2}\exp[i\vec{\sigma}\cdot(\lambda\vec{f}+2\vec{\vartheta}v)] + \tfrac{1}{2}\exp[i\vec{\sigma}\cdot(\lambda\vec{f}-2\vec{\vartheta}v)]\}\quad. \tag{25}$$

If we treat the $\vec{\sigma}$-integration as being in polar coordinates and perform the angular portion of that integration, then the exponentials each give

rise to a Bessel function according to the well known formula

$$\int_0^{2\pi} d\phi \, \exp(i \, x \cos \phi) = 2 \pi J_0(x) \qquad . \tag{26}$$

Making use of this equation, we can rewrite Eq. (25) in the form

$$\mathcal{M}(\lambda \vec{f}, \vec{\vartheta}) = \frac{8.16 \, k^2}{\pi} \int_0^z dv \, C_N^2 \int_0^\infty d\sigma \, \sigma^{-8/3} \{ 1 - J_0(\lambda f \sigma) - J_0(2 \vartheta v \sigma)$$

$$+ \tfrac{1}{2} [J_0(|\lambda\vec{f} + 2\vec{\vartheta}v| \, \sigma) + J_0(|\lambda\vec{f} - 2\vec{\vartheta}v| \, \sigma)]\} \qquad . \tag{27}$$

To proceed further, we make use of the formula[3]

$$\int_0^\infty dx \, x^\mu \, J_\nu(ax) = 2^\mu \, a^{-\mu-1} \, \frac{\Gamma(\tfrac{1}{2} + \tfrac{1}{2}\nu + \tfrac{1}{2}\mu)}{\Gamma(\tfrac{1}{2} + \tfrac{1}{2}\nu - \tfrac{1}{2}\mu)}$$

$$\text{if} \quad \text{Re} \, \nu - 1 < \text{Re} \, \mu < \tfrac{1}{2} \, , \text{ and } a > 0 \, . \tag{28}$$

Strictly speaking, this equation is not directly applicable to Eq. (27) since in our case, $\mu = 8/3$ and $\nu = 0$, so the condition $\text{Re} \, \mu > \text{Re} \, \nu - 1$ is not satisfied. There is also a problem of the divergence of the integral with 1 in place of J_0 . In fact, however, because we are dealing with a difference of factors, the σ-integration in Eq. (27) is convergent. The divergence is associated with the behavior of the integrand around $\sigma = 0$, for which $\sigma^{-8/3} J_0(\sigma x)$ clearly leads to a divergence. However, the differences are such that the quantity in the curly brackets in Eq. (27) goes as σ^2 in the vicinity of $\sigma = 0$, and so the actual dependence near $\sigma = 0$ is $\sigma^{-2/3}$. This does not have a divergence. This means that we can use Eq. (28) to evaluate Eq. (27) [with 1 replaced by $J_0(0\sigma)$] , and by an argument based on the principle of analytic continuation take the result to apply for the parameters in Eq. (27). Thus we obtain the result that

$$\mathfrak{m}(\lambda\vec{f},\vec{\vartheta}) = \frac{8.16}{\pi} \, 2^{-8/3} \, \frac{\Gamma(-5/6)}{\Gamma(11/6)} \, k^2 \int_0^z dv \, C_N^2 \, \{-(\lambda f)^{5/3} - (2\vartheta v)^{5/3}$$

$$+ \tfrac{1}{2} \, [\lambda f)^2 + 2(2\vartheta v)(\lambda f) \cos\phi + (2\vartheta v)^2]^{5/6}$$

$$+ \tfrac{1}{2} \, [(\lambda f)^2 - 2(2\vartheta v)(\lambda f) \cos\phi + (2\vartheta v)^2]^{5/6} \} \quad . \tag{29}$$

Here ϕ denotes the angle between $\vec{\vartheta}$ and $\vec{f}$.

Equation (29) represents the most general reduction of results we can carry out without making some assumption regarding the distribution of the refractive-index structure constant along the propagation path, i.e., the dependence of C_N^2 on v . In the next section, we consider the particular case corresponding to horizontal propagation for which C_N^2 is constant, independent of v .

Reduction of $\mathfrak{m}(\lambda\vec{f},\vec{\vartheta})$ for Horizontal Propagation

If we restrict attention to the case of horizontal propagation for which C_N^2 is constant, we can simplify Eq. (29) by taking C_N^2 outside the v-integration. We can then simplify the parametric dependence of the integral by making the variable of integration correspond to $2\vartheta v/\lambda f$. If we make this transformation and extract all possible parametric factors, we obtain from Eq. (29)

$$\mathfrak{m}(\lambda\vec{f},\vec{\vartheta}) = -\frac{8.16}{\pi} \, 2^{-8/3} \, \frac{\Gamma(-5/6)}{\Gamma(11/6)} \, k^2 \, \frac{(\lambda f)^{8/3}}{2\vartheta} \, C_N^2 \int_0^{f_0/f} dx \, \{1 + x^{5/3}$$

$$- \tfrac{1}{2} \, [1 + 2x \cos\phi + x^2]^{5/6} - \tfrac{1}{2} \, [1 - 2x \cos\phi + x^2]^{5/6} \} \quad . \tag{30}$$

Here we have utilized the quantity f_0 , which we call the transition image frequency, to denote

$$f_0 = 2\vartheta z/\lambda \quad . \tag{31}$$

At this point, it is interesting to seek to introduce the quantity r_0 , which measures the effect of wavefront distortion of conventional imaging. r_0 corresponds to the practical upper limit imposed by atmospheric turbulence on useful optics diameter for diffraction-limited imagery.[1] For infinite plane wave propagation, r_0 is defined by the equation

$$6.88 \; r_0^{-5/3} \; = \; 2.91 \; k^2 \; z \; C_N^2 \qquad . \tag{32}$$

This allows us to write

$$\mathcal{M}(\lambda \vec{f}, \vec{\vartheta}) = -\frac{8.16}{\pi} \; 2^{-8/3} \; \frac{\Gamma(-5/6)}{\Gamma(11/6)} \; \frac{6.88}{2.91} \; \frac{(\lambda f)^{8/3}}{2\vartheta z} \; r_0^{-5/3} \; I(f/f_0, \phi)$$

$$= -\frac{8.16}{\pi} \; 2^{-8/3} \; \frac{\Gamma(-5/6)}{\Gamma(11/6)} \; \frac{6.88}{2.91} \; \left(\frac{f}{f_0}\right)^{8/3} \left(\frac{2\vartheta z}{r_0}\right)^{5/3} \; I(f/f_0, \phi)$$

$$= 6.88 \; \left(\frac{f}{f_0}\right)^{8/3} \left(\frac{2\vartheta z}{r_0}\right)^{5/3} \; I(f/f_0, \phi) \qquad , \tag{33}$$

where

$$I(f/f_0, \phi) = \int_0^{f_0/f} dx \; \{1 + x^{5/3} - \tfrac{1}{2}[1 + 2x \cos\phi + x^2]^{5/6}$$

$$- \tfrac{1}{2}[1 - 2x \cos\phi + x^2]^{5/6} \} \qquad . \tag{34}$$

The evaluation of $\mathcal{M}(\lambda \vec{f}, \vec{\vartheta})$ reduces at this point to the evaluation of $I(f/f_0, \phi)$. In general, this integral can only be evaluated by numerical techniques, which we have performed. Before presenting the numerical results, it is appropriate to discuss the asymptotic evaluation of $I(f/f_0, \phi)$ for $f/f_0 \gg 1$ and for $f/f_0 \ll 1$. We shall denote the asymptotic form by $I_{asy}(f/f_0, \phi)$, understanding that the appropriate asymptotic form is to be used in the regions $f/f_0 < 1$ and $f/f_0 \geq 1$.

For $f/f_0 \gg 1$, x in the integrand is everywhere very small, and we can make the approximation

$$1 + x^{5/3} - \tfrac{1}{2}(1 + 2x\cos\phi + x^2)^{5/6} - \tfrac{1}{2}(1 - 2x\cos\phi + x^2)^{5/6}$$

$$\approx 1 + x^{5/3} - \tfrac{1}{2}\left[1 + \frac{5/6}{1!}(2x\cos\phi + x^2) + \frac{(5/6)(-1/6)}{2!}(2x\cos\phi)^2\right]$$

$$- \tfrac{1}{2}\left[1 + \frac{5/6}{1!}(-2x\cos\phi + x^2) + \frac{(5/6)(-1/6)}{2!}(-2x\cos\phi)^2\right]$$

$$\approx x^{5/3} - \frac{5}{6}x^2 + \frac{5}{18}x^2\cos^2\phi \qquad . \tag{35}$$

Carrying out the integration is now trivial, and we get

$$I_{asym}(f/f_0,\phi) \approx \frac{3}{8}\left(\frac{f_0}{f}\right)^{8/3}\left[1 - \frac{20}{27}\left(\frac{f_0}{f}\right)^{1/3}(1 - \tfrac{1}{3}\cos^2\phi)\right] ,$$

$$\text{if} \quad f \geq f_0 \quad . \tag{36}$$

For $f/f_0 \ll 1$, the value of the integrand in Eq. (34) is dominated by the values for which x is very much greater than unity, and we can make the approximation

$$1 + x^{5/3} - \tfrac{1}{2}(1 + 2x\cos\phi + x^2)^{5/6} - \tfrac{1}{2}(1 - 2x\cos\phi + x^2)^{5/6}$$

$$= 1 + x^{5/3} - \tfrac{1}{2}x^{5/3}\left[(1 + 2x^{-1}\cos\phi + x^{-2})^{5/6} + (1 - 2x^{-1}\cos\phi + x^{-2})^{5/6}\right]$$

$$\approx 1 + x^{5/3} - \tfrac{1}{2}x^{5/3}\left[1 + \frac{5/6}{1!}(2x^{-1}\cos\phi + x^{-2}) + \frac{(5/6)(-1/6)}{2!}(2x^{-1}\cos\phi)^2\right]$$

$$- \tfrac{1}{2}x^{5/3}\left[1 + \frac{5/6}{1!}(-2x^{-1}\cos\phi + x^{-2}) + \frac{(5/6)(-1/6)}{2!}(-2x^{-1}\cos\phi)^2\right]$$

$$\approx 1 - \frac{5}{6}x^{-1/3} + \frac{5}{18}x^{-1/3}\cos^2\phi \qquad . \tag{37}$$

- 16 -

Here again, carrying out the integration is trivial, and we get

$$I_{a\,sym}(f/f_0, \phi) \approx \left(\frac{f_0}{f}\right)\left[1 - \frac{5}{4}\left(\frac{f}{f_0}\right)^{1/3}(1 - \frac{1}{3}\cos^2\phi)\right],$$

$$\text{if} \quad f < f_0 \quad . \tag{38}$$

We have written a computer program for the evaluation of $I(f/f_0, \phi)$, and comparison of this quantity with $I_{a\,sym}(f/f_0, \phi)$. The computer program is listed in Table I.2, and the numerical results are given in Table I.3. As can be seen from these numerical results, $I_{a\,sym}(f/f_0, \phi)$ is a very good approximation to I for all values of f/f_0 when $\cos^2\phi$ is near unity, and is also a good approximation when $\cos^2\phi$ is significantly different from unity, if $f > f_0$, or less than about $0.1\, f_0$.

With these asymptotic forms, we see that Eq. (33) can be re-written as

$$\mathfrak{m}(\lambda\vec{f}, \vec{\vartheta}) \approx \begin{cases} 6.88\left(\frac{f\lambda}{r_0}\right)^{5/3}\left[1 - \frac{5}{4}\left(\frac{f}{f_0}\right)^{1/3}(1 - \frac{1}{3}\cos^2\phi)\right], & \text{if} \quad f < f_0 \\[4mm] 2.58\left(\frac{\vartheta}{\vartheta_0}\right)^{5/3}\left[1 - \frac{20}{27}\left(\frac{f_0}{f}\right)^{1/3}(1 - \frac{1}{3}\cos^2\phi)\right], & \text{if} \quad f \geq f_0 \end{cases} \tag{39}$$

where

$$\vartheta_0 = \frac{r_0}{2z}$$

The angle ϑ_0 can be considered to characterize isoplanatism for predetection compensation imaging over a horizontal path. We shall call it the critical angle for predetection compensation imaging.

In the next section, we present a discussion of the significance of our results.

Discussion of Results

If we substitute Eq. (39) into Eq. (24′), and that into Eq. (9b), we obtain the basic result that

$$\langle \tau_{PDC}(\vec{f}) \rangle = \tau_{DL}(f) \begin{cases} \exp\left\{-6.88 \left(\frac{f\lambda}{r_0}\right)^{5/3}\left[1 - \frac{5}{4}\left(\frac{f}{f_0}\right)^{1/3}\left(1 - \frac{1}{3}\cos^2\phi\right)\right]\right\} & \text{if } f < f_0 , \\[4mm] \exp\left\{-2.58 \left(\frac{\vartheta}{\vartheta_0}\right)^{5/3}\left[1 - \frac{20}{27}\left(\frac{f_0}{f}\right)^{1/3}\left(1 - \frac{1}{3}\cos^2\phi\right)\right]\right\} & \text{if } f \geq f_0 . \end{cases} \tag{41}$$

Recalling definitions given previously, we note that $\tau_{DL}(f)$ is the diffraction-limited MTF of the aperture,

$$f_0 = \frac{2\vartheta z}{\lambda} \tag{31}$$

and

$$\vartheta_0 = \frac{r_0}{2z} . \tag{40}$$

ϕ is the angle between the direction to the reference source and the orientation of the spatial frequency, $\vec{f}$, of interest.

In considering the results in Eq. (41), we note first of all that for f small compared to the transition frequency, f_0 , the MTF reduces to $\tau_{DL}(f) \exp\left[-6.88 (f\lambda/r_0)^{5/3}\right]$. If we had not used predetection compensation, the well-known long exposure result is of the form $\tau_{DL}(f) \exp\left[-3.44 (f\lambda/r_0)^{5/3}\right]$. Thus we see that for low frequencies, the MTF is actually poorer than in conventional imagery. This is apparently because for these low frequencies, the wavefront distortion compensation we are using is inappropriate. By using it, we are simply doubling the mean square wavefront error, because we are combining two independent sets of errors. This means that in practice, we must have an f_0 small enough so that $(f_0 \lambda/r_0)$ is less than unity so that the low frequencies are in a range where there is no significant wavefront distortion, and doubling the atmospheric turbulence effect will be of little consequence.

In order to get f_0 small enough, we have to have an appropriately small value for ϑ . A bit of algebraic manipulation quickly shows that the requirement that we make the transition frequency, f_0 , small enough is equivalent to the requirement that we use a reference source at an angular distance ϑ which is less than the critical angle for predetection compensation, ϑ_0 .

For image frequency f greater than the transition frequency, f_0 , we see that the predetection compensation MTF is equal to the diffraction-limited MTF, except for a factor of the order of $\exp\left[-2.58\, (\vartheta/\vartheta_0)^{5/3}\right]$. Obviously, the key to achieving a high predetection compensated MTF at high image frequencies is to use a reference source at a displacement angle ϑ which is less than the predetection compensation critical angle, ϑ_0 .

Fortunately, we get the same requirement, i.e., $\vartheta < \vartheta_0$, for good performance at both high and low image frequencies. Obviously, the magnitude of ϑ_0 is of fundamental importance, and it is interesting to see what it is for various conditions. First of all, we note from Eq. (32) that r_0 is proportional to $\lambda^{6/5}$. Considering Eq. (40), it is thus apparent that ϑ_0 is a function of wavelength, and also varies as $\lambda^{6/5}$. If we combine Eq.'s (32) and (40), we get

$$\vartheta_0 = \left(\frac{2.91}{6.88}\ 2^{5/3}\ k^2\ z^{8/3}\ C_N^2\right)^{-3/5}$$

$$= 0.0923\ \lambda^{6/5}\ z^{-8/5}\ (C_N^2)^{-3/5} \quad . \tag{42}$$

In Table I. 1, we present some representative values of the predetection compensation critical angle, ϑ_0 , along with corresponding values for the nominal angular resolution for uncompensated imagery, namely r_0 , where

$$\frac{\lambda}{r_0} = 5.42\ \lambda^{-1/5}\ z^{3/5}\ (C_N^2)^{3/5} \quad . \tag{43}$$

- 19 -

Table I. 1

Dependence of ϑ_0 and λ/r_0 For Horizontal Propagation

$$\lambda = 0.5 \, \mu m$$

$C_N^2 (m^{-2/3})$	R = 1 km		R = 3 km		R = 10 km	
	ϑ_0 (μrad)	λ/r_0 (μrad)	ϑ_0 (μrad)	λ/r_0 (μrad)	ϑ_0 (μrad)	λ/r_0 (μrad)
1×10^{-13}	2. 53	98. 7	0. 437	190. 8	0. 0637	393.
3×10^{-14}	5. 22	47. 9	0. 900	92. 6	0. 1311	190. 8
1×10^{-14}	10. 09	24. 8	1. 74	47. 9	0. 253	98. 7
3×10^{-15}	20. 8	12. 04	3. 58	23. 3	0. 522	47. 9
1×10^{-15}	40. 2	6. 23	6. 92	12. 04	1. 009	24. 8
3×10^{-16}	82. 7	3. 02	14. 27	5. 84	2. 07	12. 04
1×10^{-16}	159. 9	1. 56	27. 6	3. 02	4. 02	6. 23

It is apparent from these results that for horizontal propagation, excluding short paths with relatively light turbulence, the critical angle, ϑ_0 , is less than the nominal long exposure resolution, λ/r_0 . This means that in general, for horizontal propagation paths, predetection compensation can only be utilized if a self-referencing technique can be utilized. In general, the distortion of a resolvable distinct reference source provides incorrect predetection compensation information for imaging of a target of interest.

For vertical propagation, entirely independent calculations starting at Eq. (29) need to be carried out with an appropriate vertical distribution for the refractive-index structure constant, C_N^2 . It is likely that

in that case a simple representation involving an easily defined pre-detection compensation critical angle, ϑ_0 , and a transition frequency, f_0 , such as we have found for horizontal propagation will not apply. We intend to carry out an analysis of the vertical propagation case in a later paper. For the moment, we remark that some insight into the vertical propagation can be obtained from Table I. 1.

If we are to apply our horizontal results to the vertical propagation case, we must assume some effective height for the turbulent atmosphere. The corresponding value of C_N^2 then follows from the fact that λ/r_0 is of the order of 5×10^{-6} rad. If we assume an effective height of 1, 3, or 10 km's, the corresponding values of ϑ_0 are of the order of 40 , 14 , and 4 μrad. From this, it is apparent that unless the effective height is of the order of 1 km or less, only self-referenced predetection compensation can be utilized.

References for Chapter I

1. D. L. Fried, "Optical Resolution Through a Randomly Inhomo-
    geneous Medium for Very Long and Very Short Exposures,"
    J. Opt. Soc. Am. 56, 1372 (1966)

2. D. L. Fried, "Spectral and Angular Covariance of Scintillation
    for Propagation in a Randomly Inhomogeneous Medium,"
    Appl. Opt. 10, 721 (1971)

3. I. S. Gradshteyn and I. M. Ryzhik, "Table of Integrals, Series,
    and Products," Academic Press (New York, 1965); Eq. (14),
    Section 6.561, p. 684.

Table I.2

Computer Program Listing for Evaluation of $I(f/f_0, \phi)$ and

$I_{max}(f/f_0, \phi)$. The computer language is BASIC.

```
150 DIM A$,A$[5],B$[45]
160 LET A$="##.#"
170 LET B$="###.##   #.##^↑↑↑   #.##^↑↑↑   #.##^↑↑↑   #.###"
200 LET B=5/2
201 LET P1=1/2
202 LET P2=2/3
210 LET C=5/4
211 LET C1=2/3
212 LET C2=20/27
213 LET C3=5/4
220 READ C
221 IF C=-100 GOTO 670
230 DATA 0,.1,.2,.3,.4,.5,.6,.7,.8,.9,1,-100
240 LET C1= COS (.5*3.14159265*C)
241 LET C2=1-C1*C1/3
250 FOR Z=1 TO 35
251 PRINT
252 NEXT Z
260 PRINT  USING A$;"PHI =";C*90;" DEG."
270 FOR Z=1 TO 5
271 PRINT
272 NEXT Z
280 LET D=5E-04
290 LET I=0
300 LET X=1E-03
310 GOSUB 600
320 LET I1=K1
330 FOR L1=1 TO 5
340 FOR L2=1 TO 9
350 LET X=X+D
360 GOSUB 600
370 LET I2=K1
380 LET X=X+D
390 GOSUB 600
400 LET I3=K1
410 LET I=I+(I1+4*I2+I3)*D/3
420 LET I1=I3
425 IF X<1E-02 GOTO 480
426 IF X>100 GOTO 480
430 IF X>1 GOTO 460
440 LET J=C1*X↑P2*(1-C2*X↑P1*C2)
450 GOTO 470
```

Table 2 - Continued

```
460 LET J=M*(1-C3*C2/X+P1)
470 PRINT USING B$;X;1/X;I;J;I/J
475 IF L2=3 PRINT
480 NEXT L2
485 LET D=10*D
490 NEXT L1
500 GOTO 220
600 LET X=1-2*M*C1+M*M
610 LET X1=0
620 IF X=0 GOTO 640
630 LET X1= ABS (X)+0
640 LET X=1+2*M*C1+M*M
650 LET X1=-.5*(X1+ ABS (X)+0)+1+X+P
660 RETURN
670 STOP
680 END
```

Table I.3

Computer Printout for $I(f/f_0, \phi)$ and $I_{sys}(f/f_0, \phi)$. The output is generated by the program listed in Table 2.

THI = 0.0 DEG.

f_0/f	f/f_0	$I(f/f_0,\phi)$	$I_{sys}(f/f_0,\phi)$	I/I_{sys}
0.01	1.000E+02	1.522E-26	1.555E-26	0.979
0.02	5.000E+01	9.520E-26	9.570E-26	0.994
0.03	3.333E+01	2.752E-25	2.758E-25	0.997
0.04	2.500E+01	5.295E-25	5.332E-25	0.993
0.05	2.000E+01	1.249E-24	1.249E-24	0.999
0.06	1.666E+01	1.660E-24	1.660E-24	0.999
0.07	1.428E+01	2.434E-24	2.495E-24	0.999
0.08	1.250E+01	3.536E-24	3.507E-24	0.999
0.09	1.111E+01	4.748E-24	4.752E-24	0.999
0.10	1.000E+01	6.225E-24	6.227E-24	0.999
0.20	5.000E+00	3.647E-23	3.648E-23	0.999
0.30	3.333E+00	1.011E-22	1.012E-22	0.999
0.40	2.500E+00	2.067E-22	2.072E-22	0.997
0.50	2.000E+00	3.577E-22	3.581E-22	0.996
0.60	1.666E+00	5.540E-22	5.543E-22	0.999
0.70	1.428E+00	8.057E-22	8.134E-22	0.996
0.80	1.250E+00	1.104E-21	1.108E-21	0.996
0.90	1.111E+00	1.452E-21	1.431E-21	0.990
1.00	1.000E+00	1.844E-21	1.898E-21	0.971
2.00	5.000E-01	6.326E-21	6.771E-21	1.008
3.00	3.333E-01	1.269E+00	1.266E+00	1.002
4.00	2.500E-01	1.991E+00	1.990E+00	1.003
5.00	2.000E-01	2.564E+00	2.563E+00	1.000
6.00	1.666E-01	3.243E+00	3.243E+00	1.000
7.00	1.428E-01	3.950E+00	3.950E+00	1.000
8.00	1.250E-01	4.666E+00	4.666E+00	1.000
9.00	1.111E-01	5.394E+00	5.394E+00	0.999
10.00	1.000E-01	6.131E+00	6.132E+00	0.999
20.00	5.000E-02	1.385E+01	1.385E+01	0.999
30.00	3.333E-02	2.194E+01	2.195E+01	0.999
40.00	2.500E-02	3.022E+01	3.025E+01	0.999
50.00	2.000E-02	3.863E+01	3.868E+01	0.998
60.00	1.666E-02	4.713E+01	4.722E+01	0.997
70.00	1.428E-02	5.577E+01	5.574E+01	0.998
80.00	1.250E-02	6.451E+01	6.452E+01	0.999
90.00	1.111E-02	7.322E+01	7.326E+01	0.999
100.00	1.000E-02	8.201E+01	8.204E+01	0.999

Table 3 - Continued

PHI = 3.0 DEG.

f_0/f	f/f_0	$I(f/f_0, \phi)$	$I_{asym}(f/f_0, \phi)$	I/I_{asym}
0.01	1.000E+02	1.508E-06	1.553E-06	0.970
0.02	5.000E+01	2.470E-06	2.552E-06	0.981
0.03	3.333E+01	2.730E-05	2.750E-05	0.995
0.04	2.500E+01	5.804E-05	5.817E-05	0.997
0.05	2.000E+01	1.026E-04	1.028E-04	0.998
0.06	1.666E+01	1.662E-04	1.664E-04	0.999
0.07	1.428E+01	2.476E-04	2.478E-04	0.999
0.08	1.250E+01	3.492E-04	2.491E-04	0.999
0.09	1.111E+01	4.731E-04	4.732E-04	0.999
0.10	1.000E+01	6.001E-04	6.004E-24	0.999
0.20	5.000E+00	3.628E-03	3.630E-03	0.999
0.30	3.333E+00	1.025E-02	1.026E-02	0.999
0.40	2.500E+00	2.052E-02	2.057E-02	0.997
0.50	2.000E+00	3.546E-02	3.562E-02	0.995
0.60	1.666E+00	5.513E-02	5.554E-02	0.992
0.70	1.428E+00	7.964E-02	8.056E-02	0.988
0.80	1.250E+00	1.080E-01	1.108E-01	0.983
0.90	1.111E+00	1.409E-01	1.464E-01	0.975
1.00	1.000E+00	1.802E-01	1.375E-01	0.964
2.00	5.000E-01	6.704E-01	6.602E-01	1.014
3.00	3.333E-01	1.051E+00	1.245E+00	1.024
4.00	2.500E-01	1.770E+00	1.774E+00	1.008
5.00	2.000E-01	2.537E+00	2.533E+00	1.001
6.00	1.666E-01	3.218E+00	3.214E+00	1.001
7.00	1.428E-01	3.916E+00	3.913E+00	1.000
8.00	1.250E-01	4.698E+00	4.695E+00	1.000
9.00	1.111E-01	5.352E+00	5.350E+00	1.000
10.00	1.000E-01	6.087E+00	6.084E+00	1.000
20.00	5.000E-02	1.378E+01	1.378E+01	1.000
30.00	3.333E-02	2.194E+01	2.195E+01	0.999
40.00	2.500E-02	3.012E+01	3.013E+01	0.999
50.00	2.000E-02	3.850E+01	3.855E+01	0.998
60.00	1.666E-02	4.697E+01	4.707E+01	0.998
70.00	1.428E-02	5.560E+01	5.567E+01	0.998
80.00	1.250E-02	6.431E+01	6.433E+01	0.999
90.00	1.111E-02	7.299E+01	7.305E+01	0.999
100.00	1.000E-02	8.176E+01	8.182E+01	0.999

Table 3 - Continued

PHI = 1?.° ???.

f_0/f	f/f_0	$I(f/f_0,\phi)$	$I_{asym}(f/f_0,\phi)$	I/I_{asym}
?.?1	1.???E+??	1.5?3E-?6	1.546E-?6	?.?75
?.??	5.???E+?1	?.4??E-?6	?.4??E-?6	?.???
?.?3	3.333E+?1	?.7?4E-?5	?.7?4E-?5	?.???
?.?4	?.5??E+?1	5.761E-?5	5.775E-?5	?.??7
?.?5	?.???E+?1	1.???E-?4	1.???E-?4	?.???
?.??	1.??6E+?1	1.?4?E-?4	1.649E-?4	?.???
?.??	1.4??E+?1	?.45?E-?4	2.455E-?4	?.???
?.??	1.?5?E+?1	3.46?E-?4	3.46?E-?4	?.???
?.??	1.111E+?1	4.6??E-?4	4.6?5E-?4	?.???
?.1?	1.???E+?1	6.13?E-?4	6.13?E-?4	?.???
?.??	5.???E+??	3.575E-?3	3.577E-?3	?.???
?.3?	3.333E+??	?.?6?E-?3	?.??6'-?3	?.???
?.4?	?.5??E+??	?.???E-??	2.?15E-??	?.??6
?.5?	?.???E+??	3.45?E-??	3.4??E-??	?.???
?.6?	1.?66E+??	5.?5?E-??	5.41?E-??	?.?1?
?.??	1.4??E+??	7.???E-??	?.?61E-??	.???
?.??	1.?5??+??	1.??4?E-?1	1.??4?E-?1	?.???
?.??	1.111?+??	1.?5?E-?1	1.?17?-?1	?.?66
1.???	1.???E+??	1.7?6E-?1	1.???E-?1	?.?53
?.??	5.???E-?1	6.411E-?1	6.14?E-?1	1.?44
?.??	3.333E-?1	1.??6E+??	1.1??E+??	1.?1?
4.??	?.5??E-?1	1.???E+??	1.7??E+??	1.?11
5.??	?.???E-?1	?.466E+??	?.446E+??	1.???
6.??	1.666E-?1	3.1?6E+??	3.117E+??	1.??6
7.??	1.4??E-?1	?.3??E+??	3.3?4E+??	1.??4
?.??	1.?5?E-?1	4.5?4E+??	4.5?7E+??	1.??4
?.??	1.111E-?1	5.?4?E+??	5.???E+??	1.???
1?.??	1.???E-?1	5.?65E+??	5.?47E+??	1.???
??.??	5.???E-??	1.?5?E+?1	1.?56E+?1	1.??1
3?.??	3.33?E-??	?.15?E+?1	?.157E+?1	1.???
4?.??	?.5??E-??	?.?77E+?1	2.?7?E+?1	?.???
5?.??	?.???E-??	3.?11E+?1	3.?14E+?1	?.???
6?.??	1.666E-??	4.654E+?1	4.661E+?1	?.???
7?.??	1.4??E-??	5.51?E+?1	5.517E+?1	?.???
??.??	1.?5?E-??	6.37?E+?1	6.37?E+?1	1.???
??.??	1.111E-??	7.?4?E+?1	7.?46E+?1	?.???
1??.??	1.???E-??	?.115E+?1	?.113E+?1	?.???

Table 3 - Continued

PHI =27.0 DEG.

f_0/f	f/f_0	$I(f/f_0,\phi)$	$I_{avg}(f/f_0,\phi)$	I/I_{avg}
0.01	1.000E+02	1.430E-06	1.536E-06	0.068
0.02	5.000E+01	2.248E-06	2.417E-06	0.092
0.03	3.333E+01	2.698E-05	2.706E-05	0.996
0.04	2.500E+01	5.700E-05	5.710E-05	0.922
0.05	2.000E+01	1.015E-04	1.017E-04	0.998
0.06	1.666E+01	1.626E-04	1.627E-04	0.999
0.07	1.422E+01	2.418E-04	2.420E-04	0.999
0.08	1.250E+01	3.400E-04	3.410E-04	0.999
0.09	1.111E+01	4.628E-04	4.611E-04	0.999
0.10	1.000E+01	6.033E-04	6.036E-04	0.999
0.20	5.000E+00	2.402E-03	2.405E-03	0.999
0.30	3.333E+00	2.599E-03	2.600E-03	0.997
0.40	2.500E+00	1.041E-02	1.042E-02	0.995
0.50	2.000E+00	3.326E-02	3.358E-02	0.992
0.60	1.666E+00	5.125E-02	5.181E-02	0.987
0.70	1.422E+00	7.334E-02	7.473E-02	0.929
0.80	1.250E+00	2.023E-02	1.000E-01	0.979
0.90	1.111E+00	1.300E-01	1.342E-01	0.961
1.00	1.000E+00	1.602E-01	1.727E-01	0.848
2.00	5.000E-01	6.020E-01	5.422E-01	1.113
3.00	3.333E-01	1.142E+00	1.237E+00	0.751
4.00	2.500E-01	1.727E+00	1.622E+00	1.021
5.00	2.000E-01	2.364E+00	2.316E+00	1.022
6.00	1.666E-01	3.015E+00	2.964E+00	1.017
7.00	1.422E-01	3.697E+00	3.636E+00	1.014
8.00	1.250E-01	4.373E+00	4.323E+00	1.011
9.00	1.111E-01	5.073E+00	5.022E+00	1.010
10.00	1.000E-01	5.723E+00	5.733E+00	1.002
20.00	5.000E-02	1.297E+01	1.292E+01	1.003
30.00	3.333E-02	2.116E+01	2.112E+01	1.002
40.00	2.500E-02	2.827E+01	2.824E+01	1.000
50.00	2.000E-02	3.752E+01	3.752E+01	0.999
60.00	1.666E-02	4.537E+01	4.531E+01	0.999
70.00	1.422E-02	5.437E+01	5.438E+01	0.999
80.00	1.250E-02	6.297E+01	6.293E+01	1.000
90.00	1.111E-02	7.155E+01	7.153E+01	1.000
100.00	1.000E-02	3.022E+01	8.319E+01	1.000

Table 3 - Continued

PHI =36.7 DEG.

f_0/f	f/f_0	$I(f/f_0,\phi)$	$I_{asym}(f/f_0,\phi)$	I/I_{asym}
0.01	1.000E+02	1.472E-06	1.523E-06	0.971
0.02	5.000E+01	2.244E-06	2.314E-06	0.000
0.03	3.333E+01	2.662E-05	2.672E-05	0.996
0.04	2.500E+01	5.615E-05	5.627E-05	0.998
0.05	2.000E+01	3.306E-05	1.000E-04	0.990
0.06	1.666E+01	1.503E-04	1.503E-04	0.000
0.07	1.429E+01	2.374E-04	2.376E-04	0.999
0.08	1.250E+01	3.341E-04	3.343E-04	0.999
0.09	1.111E+01	4.514E-04	4.516E-04	0.999
0.10	1.000E+01	5.903E-04	5.907E-04	0.999
0.20	5.000E+00	3.399E-03	3.399E-03	0.999
0.30	3.333E+00	9.232E-03	9.261E-03	0.997
0.40	2.500E+00	1.859E-02	1.867E-02	0.995
0.50	2.000E+00	3.164E-02	3.191E-02	0.991
0.60	1.666E+00	4.947E-02	4.912E-02	0.986
0.70	1.428E+00	6.900E-02	7.037E-02	0.980
0.80	1.250E+00	9.322E-02	9.563E-02	0.972
0.90	1.111E+00	1.222E-01	1.248E-01	0.962
1.00	1.000E+00	1.524E-01	1.577E-01	0.953
2.00	5.000E-01	5.500E-01	4.436E-01	1.246
3.00	3.333E-01	1.072E+00	9.671E-01	1.108
4.00	2.500E-01	1.643E+00	1.537E+00	1.066
5.00	2.000E-01	2.243E+00	2.142E+00	1.047
6.00	1.666E-01	2.873E+00	2.773E+00	1.036
7.00	1.429E-01	3.523E+00	3.423E+00	1.029
8.00	1.250E-01	4.193E+00	4.092E+00	1.024
9.00	1.111E-01	4.370E+00	4.771E+00	1.020
10.00	1.000E-01	5.562E+00	5.463E+00	1.018
20.00	5.000E-02	1.823E+01	1.812E+01	1.007
30.00	3.333E-02	2.665E+01	2.656E+01	1.004
40.00	2.500E-02	2.854E+01	2.754E+01	1.000
50.00	2.000E-02	3.678E+01	3.678E+01	1.001
60.00	1.666E-02	4.502E+01	4.502E+01	1.000
70.00	1.429E-02	5.243E+01	5.243E+01	1.000
80.00	1.250E-02	6.124E+01	6.125E+01	1.001
90.00	1.111E-02	7.041E+01	7.037E+01	1.000
100.00	1.000E-02	7.803E+01	7.804E+01	1.000

Table 3 - Continued

THI =45.0 DEG.

f_0/f	f/f_0	$I(f/f_0,\phi)$	$I_{asys}(f/f_0,\phi)$	I/I_{asys}
0.01	1.000E+00	1.460E-06	1.500E-06	0.973
0.02	5.000E+01	2.115E-06	2.200E-06	0.965
0.03	3.333E+01	4.170E-06	4.320E-05	0.994
0.04	2.500E+01	5.504E-05	5.536E-25	0.997
0.05	2.000E+01	9.215E-05	9.290E-25	0.998
0.06	1.666E+01	1.567E-24	1.569E-24	0.999
0.07	1.428E+01	2.285E-04	2.327E-04	0.999
0.08	1.250E+01	3.363E-04	3.370E-04	0.999
0.09	1.111E+01	4.410E-04	4.418E-04	0.999
0.10	1.000E+01	5.741E-04	5.746E-04	0.999
0.20	5.000E+00	3.875E-03	3.878E-03	0.999
0.30	3.333E+00	2.959E-03	2.974E-03	0.999
0.40	2.500E+00	1.762E-02	1.775E-02	0.996
0.50	2.000E+00	2.322E-02	2.012E-02	0.993
0.60	1.666E+00	4.557E-02	4.603E-02	0.993
0.70	1.428E+00	6.451E-02	6.546E-02	0.985
0.80	1.250E+00	8.659E-02	8.790E-02	0.980
0.90	1.111E+00	1.115E-01	1.143E-01	0.975
1.00	1.000E+00	1.391E-01	1.435E-01	0.969
2.00	5.000E-01	5.164E-01	3.464E-01	1.490
3.00	3.333E-01	9.093E-01	8.336E-01	1.122
4.00	2.500E-01	1.530E+00	1.375E+00	1.112
5.00	2.000E-01	2.117E+00	1.984E+00	1.058
6.00	1.666E-01	2.799E+00	2.649E+00	1.053
7.00	1.428E-01	3.358E+00	3.180E+00	1.056
8.00	1.250E-01	3.995E+00	3.733E+00	1.048
9.00	1.111E-01	4.654E+00	4.432E+00	1.035
10.00	1.000E-01	5.326E+00	5.165E+00	1.031
20.00	5.000E-02	1.243E+01	1.232E+01	1.012
30.00	3.333E-02	2.000E+01	1.994E+01	1.007
40.00	2.500E-02	2.795E+01	2.791E+01	1.004
50.00	2.000E-02	3.597E+01	3.586E+01	1.003
60.00	1.666E-02	4.410E+01	4.403E+01	1.001
70.00	1.428E-02	5.240E+01	5.233E+01	1.001
80.00	1.250E-02	6.000E+01	6.066E+01	1.002
90.00	1.111E-02	6.019E+01	6.003E+01	1.001
100.00	1.000E-02	7.768E+01	7.755E+01	1.001

Table 3 - Continued

PHI =54.7 DEG.

f_0/f	f/f_0	$I(f/f_0,\phi)$	$I_{asym}(f/f_0,\phi)$	I/I_{asym}
0.01	1.000E+02	1.447E-06	1.494E-06	0.968
0.02	5.000E+01	8.985E-06	9.885E-06	0.970
0.03	3.333E+01	2.582E-05	2.594E-05	0.995
0.04	2.500E+01	5.426E-05	5.444E-05	0.996
0.05	2.000E+01	9.630E-05	9.651E-05	0.997
0.06	1.666E+01	1.535E-04	1.533E-04	0.998
0.07	1.428E+01	2.275E-04	2.277E-04	0.998
0.08	1.250E+01	3.194E-04	3.197E-04	0.999
0.09	1.111E+01	4.305E-04	4.307E-04	0.999
0.10	1.000E+01	5.617E-04	5.621E-04	0.999
0.20	5.000E+00	3.162E-03	3.163E-03	0.999
0.30	3.333E+00	8.481E-03	8.483E-03	0.999
0.40	2.500E+00	1.691E-02	1.694E-02	0.998
0.50	2.000E+00	2.826E-02	2.833E-02	0.997
0.60	1.666E+00	4.280E-02	4.294E-02	0.996
0.70	1.428E+00	6.031E-02	6.055E-02	0.995
0.80	1.250E+00	8.062E-02	8.098E-02	0.995
0.90	1.111E+00	1.035E-01	1.039E-01	0.995
1.00	1.000E+00	1.288E-01	1.292E-01	0.997
2.00	5.000E-01	4.776E-01	2.442E-01	1.955
3.00	3.333E-01	9.313E-01	6.993E-01	1.331
4.00	2.500E-01	1.444E+00	1.212E+00	1.190
5.00	2.000E-01	1.996E+00	1.765E+00	1.130
6.00	1.666E-01	2.578E+00	2.347E+00	1.098
7.00	1.428E-01	3.180E+00	2.952E+00	1.078
8.00	1.250E-01	3.806E+00	3.575E+00	1.064
9.00	1.111E-01	4.444E+00	4.214E+00	1.054
10.00	1.000E-01	5.096E+00	4.866E+00	1.047
20.00	5.000E-02	1.207E+01	1.185E+01	1.019
30.00	3.333E-02	1.954E+01	1.932E+01	1.011
40.00	2.500E-02	2.726E+01	2.706E+01	1.007
50.00	2.000E-02	3.516E+01	3.498E+01	1.005
60.00	1.666E-02	4.312E+01	4.304E+01	1.003
70.00	1.428E-02	5.137E+01	5.121E+01	1.003
80.00	1.250E-02	5.967E+01	5.946E+01	1.003
90.00	1.111E-02	6.795E+01	6.773E+01	1.003
100.00	1.000E-02	7.633E+01	7.617E+01	1.002

Table 3 - Continued

PHI =63.2 DEG.

f_0/f	f/f_0	$I(f/f_0,\phi)$	$I_{a\,sya}(f/f_0,\phi)$	$I/I_{a\,sya}$
0.01	1.000E+02	1.435E-06	1.401E-06	0.068
0.02	5.000E+01	2.003E-06	2.010E-06	1.000
0.03	3.333E+01	2.947E-05	2.947E-06	1.004
0.04	2.500E+01	5.043E-05	5.001E-06	1.008
0.05	2.000E+01	2.945E-05	2.404E-05	2.007
0.06	1.666E+01	1.527E-04	1.512E-04	2.008
0.07	1.428E+01	2.231E-04	2.233E-04	2.008
0.08	1.250E+01	3.122E-04	3.131E-04	2.000
0.09	1.111E+01	4.211E-04	4.214E-04	2.000
0.10	1.000E+01	5.430E-04	5.430E-04	2.000
2.00	5.000E+00	2.060E-03	2.060E-03	1.000
2.30	3.333E+00	2.145E-03	2.140E-03	1.000
0.40	2.500E+00	1.504E-02	1.501E-02	1.001
0.50	2.000E+00	2.601E-02	2.620E-02	1.003
0.60	1.666E+00	4.040E-02	4.015E-02	1.006
0.70	1.428E+00	5.672E-02	5.613E-02	1.010
0.80	1.250E+00	7.555E-02	7.407E-02	1.015
0.90	1.111E+00	9.670E-02	9.455E-02	1.023
1.00	1.000E+00	1.202E-01	1.163E-01	1.033
2.00	5.000E-01	4.449E-01	1.520E-01	2.926
3.00	3.333E-01	3.733E-01	5.735E-01	1.522
4.00	2.500E-01	1.362E+00	1.066E+00	1.277
5.00	2.000E-01	1.801E+00	1.526E+00	1.185
6.00	1.666E-01	2.452E+00	2.156E+00	1.137
7.00	1.428E-01	3.036E+00	2.740E+00	1.108
8.00	1.250E-01	3.620E+00	3.343E+00	1.083
9.00	1.111E-01	4.252E+00	3.963E+00	1.074
10.00	1.000E-01	4.793E+00	4.596E+00	1.064
20.00	5.000E-02	1.171E+01	1.142E+01	1.025
30.00	3.333E-02	1.395E+01	1.376E+01	1.015
40.00	2.500E-02	2.665E+01	2.638E+01	1.010
50.00	2.000E-02	3.444E+01	3.422E+01	1.007
60.00	1.666E-02	4.836E+01	4.815E+01	1.004
70.00	1.428E-02	5.045E+01	5.022E+01	1.004
80.00	1.250E-02	5.866E+01	5.832E+01	1.004
90.00	1.111E-02	6.687E+01	6.662E+01	1.003
100.00	1.000E-02	7.514E+01	7.491E+01	1.003

Table 3 - Continued

PHI =70.0 DEG.

f_0/f	f/f_0	$I(f/f_0,\phi)$	$I_{bb}(f/f_0,\phi)$	I/I_{bb}
0.01	1.000E+02	1.424E-06	1.471E-06	0.967
0.02	5.000E+01	3.016E-06	3.036E-06	0.096
0.03	3.333E+01	2.590E-05	2.538E-05	0.005
0.04	2.500E+01	5.091E-05	5.006E-05	0.007
0.05	2.000E+01	9.343E-05	9.362E-05	0.022
0.06	1.666E+01	1.486E-04	1.488E-04	0.002
0.07	1.428E+01	2.196E-04	2.108E-04	0.022
0.08	1.250E+01	3.076E-04	3.073E-04	0.000
0.09	1.111E+01	4.137E-04	4.132E-04	0.000
0.10	1.000E+01	5.337E-04	5.300E-04	0.000
0.20	5.000E+00	2.330E-03	2.070E-03	1.000
0.30	3.333E+00	7.732E-03	7.343E-03	1.002
0.40	2.500E+00	1.544E-02	1.536E-02	1.005
0.50	2.000E+00	2.560E-02	2.544E-02	1.002
0.60	1.666E+00	3.857E-02	3.794E-02	1.016
0.70	1.428E+00	5.315E-02	5.261E-02	1.005
0.80	1.250E+00	7.171E-02	6.913E-02	1.037
0.90	1.111E+00	9.169E-02	8.762E-02	1.052
1.00	1.000E+00	1.137E-01	1.063E-01	1.072
2.00	5.000E-01	4.204E-01	7.899E-02	5.324
3.00	3.333E-01	8.201E-01	4.726E-01	1.717
4.00	2.500E-01	1.299E+00	9.504E-01	1.366
5.00	2.000E-01	1.811E+00	1.461E+00	1.239
6.00	1.666E-01	2.354E+00	2.003E+00	1.174
7.00	1.428E-01	2.922E+00	2.571E+00	1.136
8.00	1.250E-01	3.519E+00	3.152E+00	1.111
9.00	1.111E-01	4.115E+00	3.763E+00	1.093
10.00	1.000E-01	4.734E+00	4.302E+00	1.000
20.00	5.000E-02	1.143E+01	1.100E+01	1.031
30.00	3.333E-02	1.766E+01	1.731E+01	1.013
40.00	2.500E-02	2.617E+01	2.594E+01	1.012
50.00	2.000E-02	3.387E+01	3.357E+01	1.033
60.00	1.666E-02	4.177E+01	4.145E+01	1.006
70.00	1.428E-02	4.972E+01	4.944E+01	1.005
80.00	1.250E-02	5.796E+01	5.753E+01	1.005
90.00	1.111E-02	6.593E+01	6.569E+01	1.004
100.00	1.000E-02	7.483E+01	7.383E+01	1.004

Table 3 - Continued

PHI =31.0 DEG.

f_0/f	f/f_0	$I(f/f_0,\phi)$	$I_{asym}(f/f_0,\phi)$	I/I_{asym}
0.01	1.000E+02	1.413E-06	1.415E-06	0.964
0.02	5.000E+01	3.736E-06	3.747E-06	0.991
0.03	3.333E+01	9.496E-06	9.514E-06	0.998
0.04	2.500E+01	5.931E-05	5.954E-05	0.995
0.05	2.000E+01	9.054E-05	9.072E-05	0.997
0.06	1.666E+01	1.471E-04	1.473E-04	0.998
0.07	1.428E+01	2.173E-04	2.175E-04	0.998
0.08	1.250E+01	3.042E-04	3.045E-04	0.999
0.09	1.111E+01	4.088E-04	4.091E-04	0.999
0.10	1.000E+01	5.302E-04	5.304E-04	0.999
0.20	5.000E+00	2.922E-03	2.925E-03	1.001
0.30	3.333E+00	7.714E-03	7.695E-03	1.002
0.40	2.500E+00	1.506E-02	1.464E-02	1.023
0.50	2.000E+00	2.490E-02	2.461E-02	1.014
0.60	1.666E+00	3.741E-02	3.459E-02	1.024
0.70	1.428E+00	5.003E-02	5.026E-02	1.037
0.80	1.250E+00	6.230E-02	6.536E-02	1.054
0.90	1.111E+00	7.250E-02	7.902E-02	1.075
1.00	1.000E+00	1.007E-01	3.040E-02	1.170
2.00	5.000E-01	4.951E-01	3.120E-02	*.***
3.00	3.333E-01	9.016E-01	4.211E-01	1.963
4.00	2.500E-01	1.850E+00	9.759E-01	1.438
5.00	2.000E-01	1.760E+00	1.374E+00	1.280
6.00	1.666E-01	2.600E+00	1.906E+00	1.668
7.00	1.428E-01	2.950E+00	2.463E+00	1.152
8.00	1.250E-01	3.490E+00	3.000E+00	1.107
9.00	1.111E-01	4.100E+00	3.098E+00	1.100
10.0	1.000E-01	4.530E+00	3.945E+00	1.001
20.00	5.000E-02	1.195E+01	1.006E+01	1.035
30.00	3.333E-02	1.841E+01	1.302E+01	1.021
40.00	2.500E-02	2.536E+01	2.549E+01	1.014
50.00	2.000E-02	3.351E+01	3.317E+01	1.010
60.00	1.666E-02	4.130E+01	4.099E+01	1.007
70.00	1.428E-02	4.865E+01	4.804E+01	1.006
80.00	1.250E-02	5.735E+01	5.690E+01	1.006
90.00	1.111E-02	6.543E+01	6.510E+01	1.005
100.00	1.000E-02	7.353E+01	7.300E+01	1.004

Table 3 - Continued

f_0/f	f/f_0	$I(f/f_0,\phi)$	$I_{asym}(f/f_0,\phi)$	I/I_{asym}
0.01	1.000E+02	1.399E-06	1.462E-06	0.956
0.02	5.000E+01	3.676E-06	3.889E-06	0.989
0.03	3.333E+01	2.484E-05	2.508E-05	0.990
0.04	2.500E+01	5.206E-05	5.239E-05	0.993
0.05	2.000E+01	9.209E-05	9.251E-05	0.995
0.06	1.666E+01	1.464E-04	1.469E-04	0.996
0.07	1.428E+01	2.162E-04	2.169E-04	0.997
0.08	1.250E+01	3.027E-04	3.033E-04	0.997
0.09	1.111E+01	4.068E-04	4.075E-04	0.998
0.10	1.000E+01	5.294E-04	5.311E-04	0.998
0.20	5.000E+00	2.910E-03	2.907E-03	1.001
0.30	3.333E+00	7.655E-03	7.624E-03	1.004
0.40	2.500E+00	1.482E-02	1.479E-02	1.002
0.50	2.000E+00	2.473E-02	2.433E-02	1.016
0.60	1.666E+00	3.701E-02	3.603E-02	1.027
0.70	1.428E+00	5.165E-02	4.959E-02	1.041
0.80	1.250E+00	6.850E-02	6.460E-02	1.060
0.90	1.111E+00	8.744E-02	8.064E-02	1.084
1.00	1.000E+00	1.083E-01	9.726E-02	1.114
2.00	5.000E-01	4.002E-01	1.574E-02	*.***
3.00	3.333E-01	7.022E-01	3.398E-01	1.931
4.00	2.500E-01	1.246E+00	3.501E-01	1.465
5.00	2.000E-01	1.743E+00	1.344E+00	1.295
6.00	1.666E-01	2.271E+00	1.872E+00	1.213
7.00	1.428E-01	2.826E+00	2.425E+00	1.164
8.00	1.250E-01	3.402E+00	3.000E+00	1.133
9.00	1.111E-01	3.992E+00	3.591E+00	1.111
10.00	1.000E-01	4.599E+00	4.108E+00	1.095
20.00	5.000E-02	1.119E+01	1.073E+01	1.037
30.00	3.333E-02	1.832E+01	1.792E+01	1.022
40.00	2.500E-02	2.575E+01	2.537E+01	1.014
50.00	2.000E-02	3.339E+01	3.303E+01	1.010
60.00	1.666E-02	4.115E+01	4.084E+01	1.007
70.00	1.428E-02	4.912E+01	4.876E+01	1.006
80.00	1.250E-02	5.719E+01	5.679E+01	1.007
90.00	1.111E-02	6.526E+01	6.489E+01	1.005
100.00	1.000E-02	7.349E+01	7.306E+01	1.004

- 35 -

CHAPTER II

A New Model for the Vertical Distribution
of the Optical Strength of Turbulence in

the Atmosphere

Presentation

It is the objective of this chapter to present a plausible model for the vertical distribution of the refractive-index structure constant $C_N{}^2(h)$ as a function of altitude, h, based on the most current available atmospheric turbulence data. The actual distribution is, of course, stochastic, and very likely varies to some extent with geographic location. However, our objective here is merely to obtain a reasonable model which can be used to carry out order-of-magnitude type calculations of the optical effects of atmospheric turbulence. With this objective in mind, we recognize that not only is it not possible for us to retain the details of fine scale dependence of $C_N{}^2$ on h which might be observed at any instant of time, but also it is neither appropriate nor significant to do so. The detailed atmospheric physics which can result in order-of-magnitude changes in $C_N{}^2$ when h changes less than 1 km, at some high altitude, is obviously of potential interest to the atmospheric physicist who wishes to study the mechanism by which refractive-index variations are generated in the atmosphere. However, for those of us who merely wish to carry out optical effects calculations, since the weighting factors are relatively slowly and smoothly varying factors of position along the propagation path, it is only necessary to develop an estimate of the average value of $C_N{}^2$ in each altitude regime. Although actual values of $C_N{}^2$ versus altitude, h, may show spikes, as depicted in Fig. II.1, it is entirely permissible for us to smooth the data so long as we retain the correct integrated value of $C_N{}^2$ in each altitude regime.

The absence of direct optical data from which the distribution of $C_N{}^2$ versus h could be developed forces us to rely on thermal probe measurements of the temperature structure constant, $C_T{}^2$, from which the refractive-index structure constant, $C_N{}^2$, can be calculated. For this purpose, we have found it convenient to utilize the balloon flight data gathered by Bufton[1] for the altitude regime between 500 m and 20,000 m,

- 37 -

and the airplane flight data of Koprov and Tsvang[2] for the altitude regime between 50 m and 500 m. (It is, in fact, the recent availability of Bufton's high altitude data that makes the development of this new turbulence distribution model practical and appropriate.)

The Koprov and Tsvang data, because it represents level flight at each altitude, gives a reasonable average value and so relatively little data smoothing is required. Their data, representing the average of seven day time flights, and the average of five night time flights, is shown in Fig.II. 2. The solid lines show a fit to the data according to the equations

$$C_N^2(h) = 6.5 \times 10^{-14} \, h^{-1} \, , \quad 50 < h < 500 \text{ m} \quad \text{(day time)} \tag{1a}$$

$$C_N^2(h) = \begin{cases} 7.0 \times 10^{-14} \, h^{-4/3} \, , & 50 < h < 100 \text{ m} \\ 1.5 \times 10^{-18} & , \quad 100 < h < 500 \text{ m} \end{cases} \quad \text{(night time)} \tag{1b}$$

where C_N^2 is in units of $m^{-2/3}$ and h is in units of m .

The balloon flight data of Bufton represents four night time flights. Using the integrated measured values[3] of C_N^2 (derived from C_T^2) and smoothing the data to suppress sharp altitude dependence, we have calculated the average value of C_N^2 in 1 km altitude increments centered at 1 km, 2 km, 3 km, etc., up to 20 km, for each of the four flights. The results are shown in Table II. 1, along with the average value for all four flights. These values are depicted in Fig. II. 3.

Rather than slavishly follow the detailed variations of these data points, we have reasoned that the sharp variations we see in Fig. II. 3 are the result of only having four data sets to average over. We assume that the real dependence in a statistical average sense is an altitude regime dependence, and have therefore utilized the much smoother curve shown

to approximate what we believe the data says is the actual statistical average altitude dependence. The corresponding adjusted set of values for C_N^2 is listed in Table II. 2.

We consider Eq.'s (1a and 1b) and the data in Table II. 2 to represent our model for the altitude dependence of the refractive-index structure constant.

It is interesting to note that this model bears a qualitatively striking relationship to that proposed by Hufnagel[4], particularly in terms of the excess turbulence in the 10 km to 15 km altitude range, although the values we have appear to be smaller than those of Hufnagel's model. However, this may merely be a consequence of our decision to smooth over altitude. (It is difficult to be more quantitative in the comparison, because of the problem of estimating the altitude range for the disturbed layers in Hufnagel's model.)

As a check on our model for C_N^2, we have calculated the value of the critical coherence length, r_0, and the log-amplitude variance, σ_ℓ^2, for $\lambda = 0.55 \, \mu m$ and vertical propagation, according to the equations

$$ r_0 = \left\{ \frac{2.91}{6.88} \left(\frac{2\pi}{\lambda} \right)^2 \int_{Path} dh \; C_N^2(h) \right\}^{-3/5} , \tag{2} $$

and

$$ \sigma_\ell^2 = 0.56 \left(\frac{2\pi}{\lambda} \right)^{7/6} \int_{Path} dh \; h^{5/6} \; C_N^2(h) . \tag{3} $$

We calculate that r_0 should equal 0. 095 m in the day time and 0. 100 m at night. Calculations of σ_ℓ^2 give essentially the same result for both day and night, namely 0. 116 neper^2. The night time r_0 result is to be

- 39 -

compared with measured values[5] centered around 0.114 m . This agreement is excellent. The σ_ℓ^2 value is to be compared with measurements[6] near the zenith giving values of .050 ± .019 nepers^2 . The agreement is hardly outstanding, but seems reasonable considering the uncertainties of the quantities involved and of the limited size of the samples available.

References for Chapter II

1. J. L. Bufton, "Comparison of Vertical Profile Turbulence Structure with Stellar Observations," Appl. Opt. 12, 1785 (1973)

2. V. M. Koprov and L. R. Tsvang, "Characteristics of Very Small-Scale Turbulence in a Stratified Boundary Layer," Atmos. and Oceanic Phys. 22, 1142 (1966) (English translation journal, page 705)

3. We are indebted to Mr. Bufton for making tables of integrated flight data available to us.

4. R. E. Hufnagel, "An Improved Model Turbulent Atmosphere," in Appendix 3 of "Restoration of Atmospherically Degraded Images," Vol. 2, Woods Hole Summer Study, July 1966, published by the National Academy of Science.

5. D. L. Fried and G. E. Mevers, "Evaluation of r_0 for Propagation Down Through the Atmosphere," Optical Science Consultants Report No. TR-120

6. J. J. Burke, "Observations of the Wavelength Dependence of Stellar Scintillation," J. Opt. Soc. Am. 60, 1262 (1970)

Table II. 1

Bufton's Flight Data -- Smoothed and Averaged

The data shown here is based on smoothing the raw data over 1000 m altitude increments. This is accomplished by using the altitude integrated measured values of C_N^2. We plot this data, passing a reasonably smooth curve through the results, and then determine the change in the integrated value, as represented by the curve, over 1000 m increments. Each 1000 m interval is centered at an exact number of km altitude. Thus the intervals are 0.5 km to 1.5 km, called the 1 km altitude interval, 1.5 km to 2.5 km, called the 2 km altitude interval, etc. A single average value of C_N^2 for each interval is then calculated from the change in the integrated value.

Alt. (km)	Refractive-Index Structure Constant, $C_N^2(h) \times 10^{16}$, $(m^{-2/3})$				
	Flt. #4	Flt. #6	Flt. #7	Flt. #9	Avg. (4 Flts.)
1	0.47	0.35	0.39	0.65	0.465
2	0.15	1.90	1.74	1.25	1.260
3	0.19	0.75	0.76	0.40	0.525
4	0.23	0.14	1.57	0.76	0.675
5	0.17	0.87	0.10	0.20	0.335
6	0.27	0.23	0.00	0.26	0.190
7	0.31	0.24	0.00	0.33	0.220
8	0.38	0.21	0.00	0.41	0.250
9	0.46	0.17	0.00	0.57	0.300
10	0.55	0.14	0.60	0.78	0.518
11	0.50	0.13	0.01	1.00	0.410
12	0.42	0.13	0.18	0.67	0.350
13	0.38	0.50	0.40	0.47	0.438
14	0.26	1.27	0.18	0.34	0.513
15	0.23	0.27	0.13	0.26	0.223
16	0.19	0.10	0.11	0.21	0.153
17	0.22	0.08	0.08	0.13	0.128
18	0.20	0.02	0.02	0.12	0.090
19	0.20	0.00	0.04	0.06	0.075
20	0.20	0.00	0.07	0.05	0.080

Table II. 2

Bufton's Flight Data -- Adjusted Averages

In plotting in Fig. II. 3 the average flight data from Table II. 1, we have noted certain fairly obvious anomalies. We believe these anomalies are artifacts due to the limited statistical sample, i. e., the use of data from only four flights.   These anomalies have been eliminated in the adjusted averages by some fairly minor redistribution of values of C_N^2 .   The adjusted values shown in this table correspond to the curve shown in Fig. II. 3. An asterisk (*) indicates an adjusted value that deviates from the average value in Table II. 1.

Altitude h , (km)	Refractive-Index Structure Constant $C_N^2 \times 10^{16}$, $(m^{-2/3})$
1	0. 465
2	1. 260
3	0. 675 *
4	0. 525 *
5	0. 335
6	0. 190
7	0. 220
8	0. 250
9	0. 300
10	0. 395 *
11	0. 460 *
12	0. 510 *
13	0. 475 *
14	0. 385 *
15	0. 223
16	0. 153
17	0. 128
18	0. 090
19	0. 075
20	0. 080
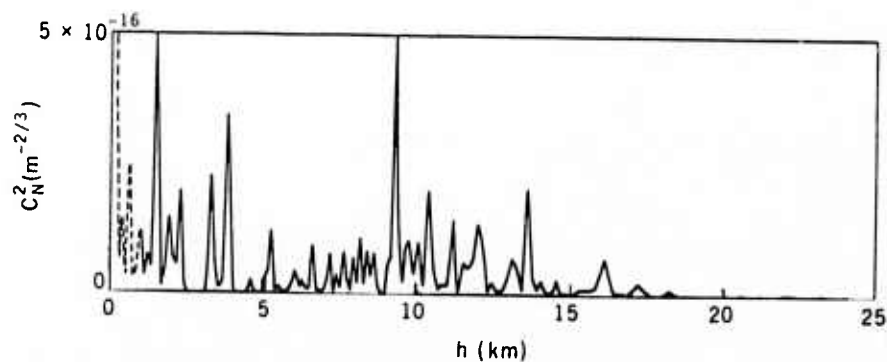
Figure II. 1. Bufton's[1] Thermal Probe Data, Flight #9

The values of C_N^2 computed from the thermal probe
data are shown without any altitude smoothing.   The
spikiness of the data is so severe as to make use of
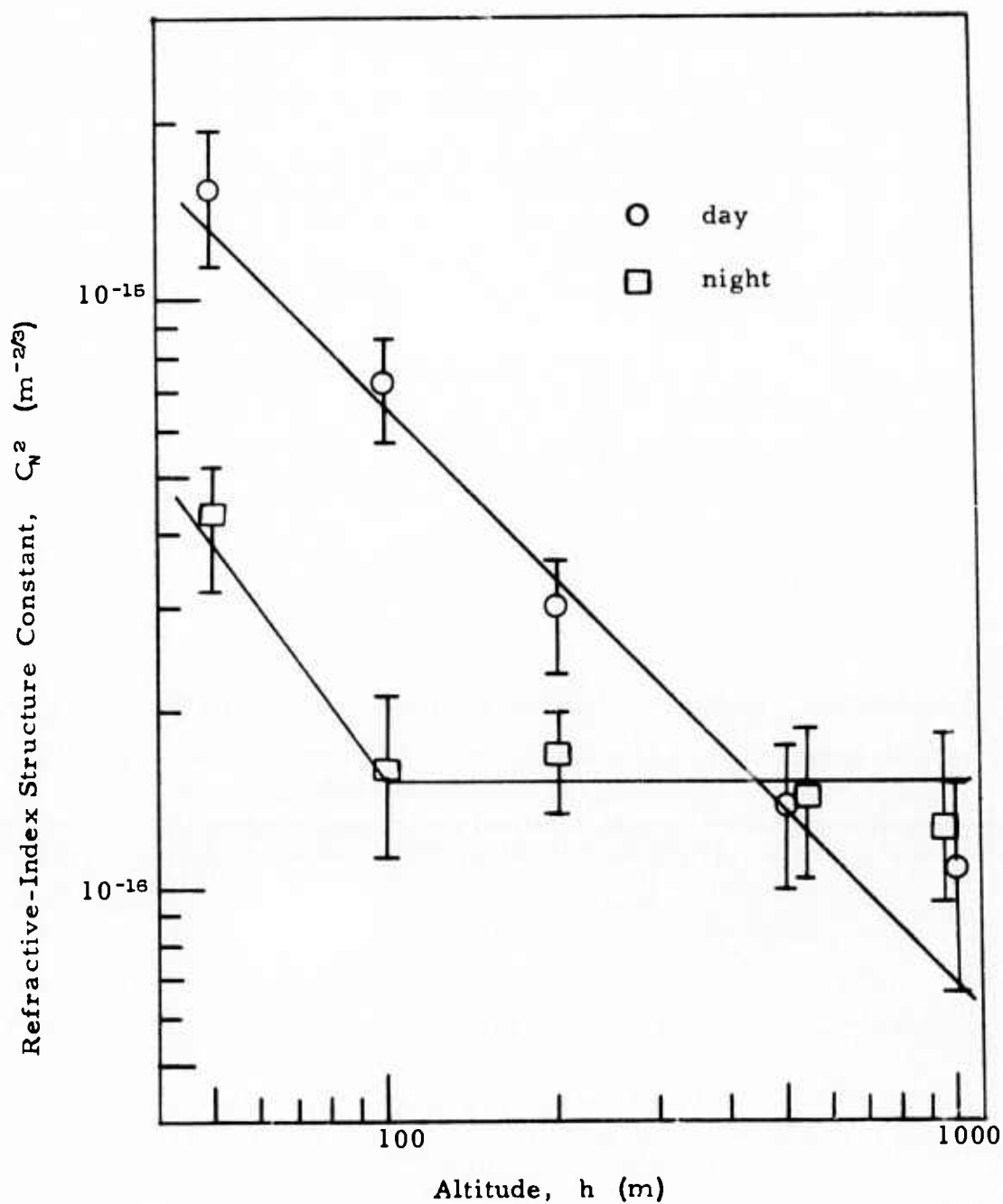the data for calculation of atmospheric optical effects
rather difficult.

Figure II.2. Low Altitude Thermal Probe Measurement of the Refractive-Index Structure Constant. The data is extracted from the airplane flight data of Koprov and Tsvang.[2]
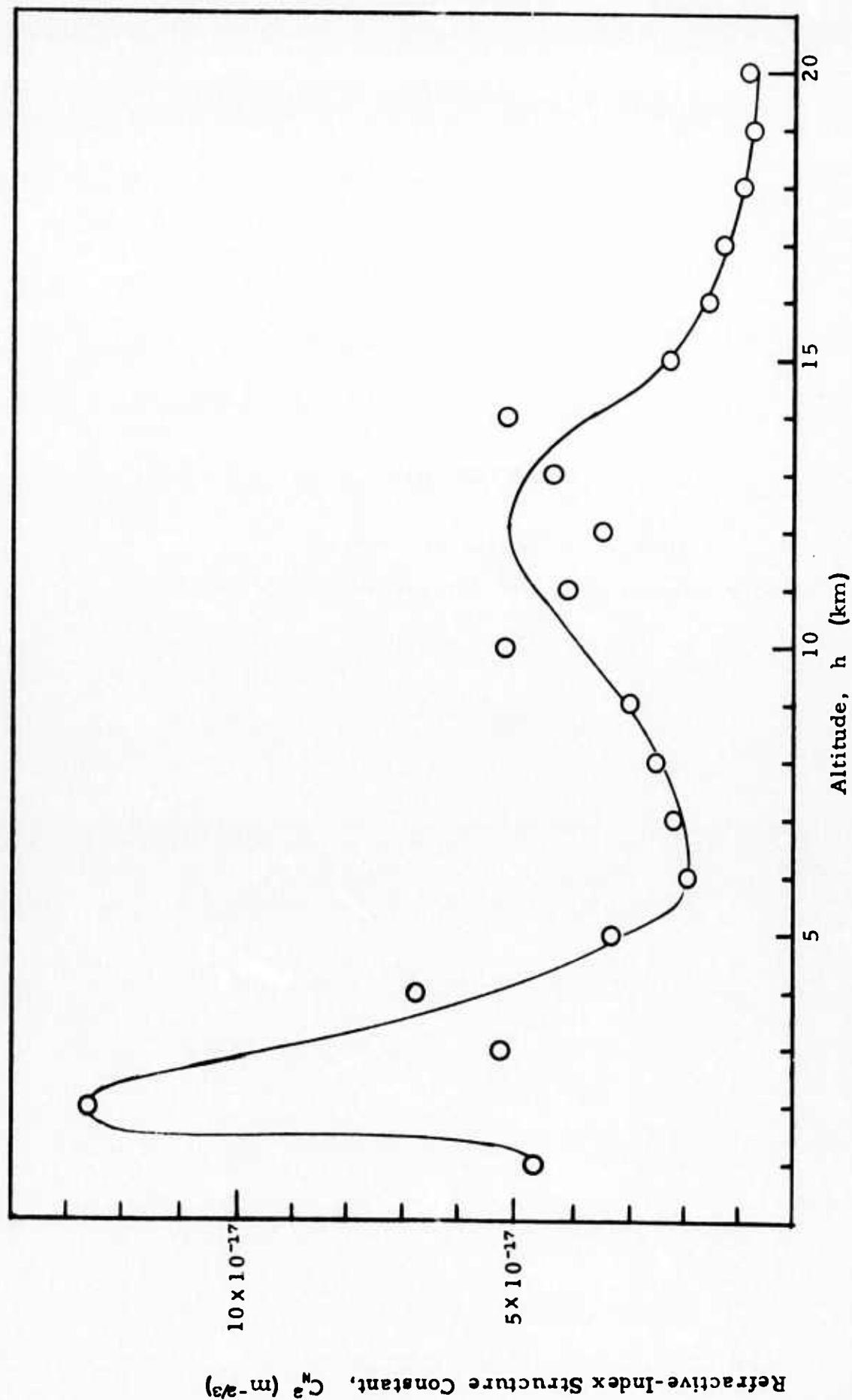
Figure II.3. High Altitude Thermal Probe Measurement of the Refractive-Index Structure Constant. The data is extracted, by smoothing and adjusting the balloon flight data of Bufton.[1] The circles represent the averages in Table II.1, and the curve represents the adjusted data in Table II.2.

- 45 -

CHAPTER III

Differential Angle of Arrival:
Theory, Evaluation, and Measurement Feasibility

Introduction

In this chapter, we are concerned with the problem of developing theoretical results for the mean-square difference in angle-of-arrival of light seen through two small but finite apertures viewing the same point source. The two apertures are separated by a distance which is a few times the diameter of each aperture. We wish to calculate the magnitude of the mean-square angle difference as a function of the separation.

Our interest in this problem is related to an experimental problem. Ideally, we would like to make measurements of the phase difference between the two apertures when viewing a monochromatic point source (i.e., a laser). This would give us a direct handle on measurement of the phase structure function, which because of its relationship to the atmospheric turbulence limited imaging problem, is of direct interest to us. For measurements of propagation paths between two points on the ground, it is a practical matter to undertake mean-square phase difference measurements. However, when the source is off the ground, as it must be if we are to be able to make measurements of propagation over non-horizontal paths, making mean-square phase difference measurements is not practical. For such a measurement, the receiver will have to track the source and any angular tracking error (with a component in the plane defined by the line-of-sight and the line-of-separation of the two apertures) will produce a phase difference. This phase difference will appear to be the same as a propagation-induced phase difference. Unless the tracking is virtually perfect, the measurement results will be dominated by this tracking error, leading to basically spurious conclusions.

In order to avoid this measurement problem and yet get a handle on the measurement of phase differences, one's attention is then naturally directed to the possibilities offered by making angle-of-arrival measurements. The angle of arrival is basically the first derivative of the phase

difference and we should be able to extract phase difference statistics information from angle-of-arrival statistics.

Actually, the basic angle-of-arrival measurements are plagued by the same tracking error problem as is the phase-difference measurements. Tracking error effects are potentially indistinguishable from propagation-induced angle-of-arrival fluctuations. However, by working with the difference in angle-of-arrival at two separated apertures mounted on the same tracking assembly, and calculating the mean-square value of this difference (rather than the covariance of angle-of-arrival at the two apertures, for example), we avoid any effect due to tracking error. The tracking error is the same for the two apertures, and its contribution drops out of the difference of angle-of-arrival at the two apertures. Hence our interest in studying the expected value of the mean-square difference of angle-of-arrival at two apertures as a function of the separation of the apertures. This problem provides the theoretical framework for a practical measurement of effects related to phase distortion over a non-horizontal propagation path.

In the next section, we define the measurement problem in terms of the applicable parameters and then set up the mathematical formulation of the problem in a tractable form. In the section following that, we carry out the necessary analysis to reduce our formulation to a two-dimensional definite integral which can be evaluated on a digital computer. In the section after that, we present the computer evaluation procedure and results. The final section presents a brief discussion of these results and their implication in terms of required angular measurement precision.

We have also included an appendix which briefly sets forth an alternate approach to this evaluation problem based on the assumption that the apertures are very small and that the angle-of-arrival can be considered to be simply the derivative of the phase. We show that this approach runs into divergence difficulties which can be lifted by introduction

of the inner scale of turbulence. We argue, however, that this divergence is more properly lifted by the finite size of the measurement aperture, and that a theory which does not take this into account should not be considered applicable for finite sized apertures.

Problem Definition and Formulation

We have previously shown[1] that over a circular region of diameter D, a distorted wavefront, represented by the random function $\phi(\vec{x})$, can be conveniently decomposed into a set of terms each of which represents some geometric aspect of the wavefront distortion. In order to accomplish this decomposition, a set of orthonormal (two-dimensional polynomial) functions, $F_i(\vec{x})$, were defined. These functions were directly related to the Zernike polynomials. Of particular interest to us here are the two functions which are related to tilt along the two orthogonal component directions in the $\vec{x}$-plane. If we denote the two components of $\vec{x}$ by (x, y), then these two functions are

$$F_{tilt}(\vec{x}) = \left(\frac{64}{\pi D^4}\right)^{\frac{1}{2}} x \; ; \; \text{and} \; \left(\frac{64}{\pi D^4}\right)^{\frac{1}{2}} y \; . \tag{1}$$

The coefficient a_{tilt} is obtained from the equation

$$a_{tilt} = \int d\vec{x} \; W(\vec{x}, D) \; F_{tilt}(\vec{x}) \; \phi(\vec{x}) \quad , \tag{2}$$

where the integration is over the infinite $\vec{x}$-plane with the actual region of integration limited by the circular aperture function $W(\vec{x}, D)$, defined by the equation

$$W(\vec{x}, D) = \begin{cases} 1 & \text{if } |\vec{x}| \leq \frac{1}{2} D \\ 0 & \text{if } |\vec{x}| > \frac{1}{2} D \end{cases} \quad . \tag{3}$$

In order to extract the tilt angle, α from a_{tilt}, we need a scaling factor. We obtain this factor by noting that when $\phi(\vec{x})$ is replaced by x

(or y), we expect the slope to be unity, and by noting that the slope associated with the phase function, $\phi(\vec{x})$, should be calculated from the isophase height function $(\lambda/2\pi)\phi(\vec{x})$. Since

$$\int d\vec{x}\ W(\vec{x}, D)\left\{\left(\frac{64}{\pi D^4}\right)^{\frac{1}{2}} x\right\} x = \left(\frac{\pi D^4}{64}\right)^{\frac{1}{2}} \quad , \tag{4}$$

it follows that the normalization factor is $(\lambda/2\pi)(\pi D^4/64)^{-\frac{1}{2}}$. This means that the tilt angle α associated with the random phase function $\phi(\vec{x})$ over a circular aperture of diameter D is

$$\alpha = \frac{\lambda}{2\pi}\left(\frac{64}{\pi D^4}\right)^{\frac{1}{2}} \int d\vec{x}\ W(\vec{x}, D)\ F_{tilt}(\vec{x})\ \phi(\vec{x}) \quad . \tag{5}$$

The experimental set-up whose results we wish to analyze concerns a pair of circular apertures each of diameter D , with their centers at $\vec{x}_1$ and $\vec{x}_2$. The difference of the angle-of-arrival components along the x-axis, as seen through these two apertures, can be written in accordance with Eq.'s (1) and (5) as

$$\alpha_1 - \alpha_2 = \frac{32\ \lambda}{\pi^2 D^4} \int d\vec{x}\ W(\vec{x}, D)\ x\ [\phi(\vec{x}_1 + \vec{x}) - \phi(\vec{x}_2 + \vec{x})] \quad . \tag{6}$$

We can write the square of $\alpha_1 - \alpha_2$ as the product of two integrals, and that as a double integral over $\vec{x}$ and $\vec{x}'$. Then by taking advantage of the fact that we can commute the processes of integration and ensemble averaging (which we denote by the angle brackets, $\langle\ \rangle$), we see that we can write the mean-square angle-of-arrival x-component difference as

$$\langle(\alpha_1 - \alpha_2)^2\rangle = \left(\frac{32\ \lambda}{\pi^2 D^4}\right)^2 \iint d\vec{x}\ d\vec{x}'\ W(\vec{x}, D)\ W(\vec{x}', D)\ x\ x'$$

$$\times\ \langle[\phi(\vec{x}_1 + \vec{x}) - \phi(\vec{x}_2 + \vec{x})][\phi(\vec{x}_1 + \vec{x}') - \phi(\vec{x}_2 + \vec{x}')]\rangle \quad . \tag{7}$$

This equation represents our basic problem formulation. In the next section we shall turn our attention to the reduction of this formulation to a numerically evaluatable result.

Formulation Reduction

At this point, it is convenient to make the change of variables from $\vec{x}$, $\vec{x}'$ to the difference and sum variables, $\vec{u}$, $\vec{v}$, where

$$\vec{u} = \vec{x} - \vec{x}' \quad , \tag{8}$$

$$\vec{v} = \tfrac{1}{2}(\vec{x} + \vec{x}') \quad . \tag{9}$$

The ensemble average in Eq. (7) can now be written in terms of the four product terms expressed as phase covariances, as $C_\phi(\vec{u}) - C_\phi(\vec{x}_2 - \vec{x}_1 + \vec{u})$ $- C_\phi(\vec{x}_2 - \vec{x}_1 - \vec{u}) + C_\phi(\vec{u})$. However, by adding and subtracting twice the phase variance and appropriately grouping terms, making use of the fact that the structure function for a stationary random variable is twice the difference of variance and covariance, we can more conveniently rewrite the ensemble average in Eq. (7) in terms of this phase-structure function, as $\tfrac{1}{2} \mathcal{D}_\phi(\vec{x}_2 - \vec{x}_1 + \vec{u}) + \tfrac{1}{2} \mathcal{D}_\phi(\vec{x}_2 - \vec{x}_1 - \vec{u}) - \mathcal{D}_\phi(\vec{u})$.

If we introduce the vector $\vec{S}$ to represent the center-to-center separation of the two apertures, i.e.,

$$\vec{S} = \vec{x}_2 - \vec{x}_1 \quad , \tag{10}$$

then we can rewrite Eq. (7) as

$$\langle (\alpha_1 - \alpha_2)^2 \rangle = \left(\frac{32\,\lambda}{\pi^2 D^4}\right)^2 \iint d\vec{u}\; d\vec{v}\; (\vec{v} + \tfrac{1}{2}\vec{u})_x\; (\vec{v} - \tfrac{1}{2}\vec{u})_x\; W(\vec{v} + \tfrac{1}{2}\vec{u}, D)\; W(\vec{v} - \tfrac{1}{2}\vec{u}, D)$$
$$\times\; [\tfrac{1}{2}\mathcal{D}_\phi(\vec{S} + \vec{u}) + \tfrac{1}{2}\mathcal{D}_\phi(\vec{S} - \vec{u}) - \mathcal{D}_\phi(\vec{u})] \quad . \tag{11}$$

In the above, the subscript x is used to denote that only the component along the x-axis is to be considered.

If we now introduce the function $K(\vec{u}, D)$, where

$$K(\vec{u}, D) = \int d\vec{v}\; (\vec{v} + \tfrac{1}{2}\vec{u})_x\; (\vec{v} - \tfrac{1}{2}\vec{u})_x\; W(\vec{v} + \tfrac{1}{2}\vec{u}, D)\; W(\vec{v} - \tfrac{1}{2}\vec{u}, D) \quad , \tag{12}$$

then we can rewrite Eq. (11) as

$$\langle (\alpha_1 - \alpha_2) \rangle = \left(\frac{32 \lambda}{\pi^2 D^4} \right)^2 \int d\vec{u} \ K(\vec{u}, D) \ [\tfrac{1}{2} \mathcal{D}_\phi (\vec{S} + \vec{u}) + \tfrac{1}{2} \mathcal{D}_\phi (\vec{S} - \vec{u}) - \mathcal{D}_\phi (\vec{u})] . \tag{13}$$

We now turn our attention to carrying out the two-dimensional integral in Eq. (12).

To carry out the integral in Eq. (12), it is convenient to represent the vector $\vec{v}$ by the two components (p, q) , where the p-axis is taken to be parallel to $\vec{u}$. We shall let θ denote the angle between the x-axis and $\vec{u}$. We can then write

$$(\vec{v} \pm \tfrac{1}{2} \vec{u})_x = p \cos \theta - q \sin \theta \pm \tfrac{1}{2} u \cos \theta . \tag{14}$$

The integration limits imposed by the two W-functions in Eq. (12) are such that we can now write

$$K(\vec{u}, D) = 2 \int_{0}^{(D-u)/2} dp \int_{-[(D/2)^2-(p+u/2)^2]^{1/2}}^{+[(D/2)^2-(p+u/2)^2]^{1/2}} dq \ [p^2 \cos^2 \theta - 2pq \cos \theta \sin \theta + q^2 \sin^2 \theta$$
$$- (\tfrac{1}{2} u)^2 \cos^2 \theta] . \tag{15}$$

By regrouping and adding and subtracting various quantities, this can be rewritten as

$$K(\vec{u}, D) = 2 \int_{0}^{(D-u)/2} dp \int_{-[(D/2)^2-(p+u/2)^2]^{1/2}}^{+[(D/2)^2-(p+u/2)^2]^{1/2}} dq \ [(p + \tfrac{1}{2}u)^2 \cos^2 \theta - (p + \tfrac{1}{2}u) u \cos^2 \theta$$
$$- 2 (p + \tfrac{1}{2}u) q \cos \theta \sin \theta + q u \cos \theta \sin \theta + q^2 \sin^2 \theta] \tag{16}$$

It is convenient here to make a change of variable so that $(p + \tfrac{1}{2}u)$ is replaced by p . With this change of variable, we can rewrite Eq. (16) as

- 52 -

$$K(\vec{u}, D) = 2 \int_{u/2}^{D/2} dp \int_{-[(D/2)^2-p^2]^{1/2}}^{+[(D/2)^2-p^2]^{1/2}} dq \ (p^2 \cos^2 \theta - pu \cos^2 \theta - 2pq \cos \theta \sin \theta$$

$$+ qu \cos \theta \sin \theta + q^2 \sin^2 \theta) \quad . \tag{17}$$

Carrying out the q-integration is a trivial process. We obtain

$$K(\vec{u}, D) = 4 \int_{u/2}^{D/2} dp \ \{p^2 [(\tfrac{1}{2} D)^2 - p^2]^{\frac{1}{2}} \cos^2 \theta - p[(\tfrac{1}{2} D)^2 - p^2]^{\frac{1}{2}} \cos^2 \theta$$

$$+ \tfrac{1}{3} [(\tfrac{1}{2} D)^2 - p^2]^{3/2} \sin^2 \theta \} \quad . \tag{18}$$

Now if we extract a factor of $(\tfrac{1}{2} D)^4$ from inside the integral in Eq. (18) and make a further change of the variable of integration, replacing $p/(\tfrac{1}{2} D)$ by p , we get

$$K(\vec{u}, D) = 4 (\tfrac{1}{2} D)^4 \int_{u/D}^{1} dp \ \{p^2 (1-p^2)^{\frac{1}{2}} \cos^2 \theta - 2p(1-p^2)^{\frac{1}{2}} (u/D) \cos^2 \theta$$

$$+ \tfrac{1}{3} (1-p^2)^{3/2} \sin^2 \theta \} \quad . \tag{19}$$

The integrations in Eq. (19) can be carried out in terms of the formulas given by Dwight[2]. We can write

$$K(\vec{u}, D) = \tfrac{1}{4} D^4 \Big(\{\tfrac{1}{8} \cos^{-1} (u/D) + [1 - (u/D)^2]^{\frac{1}{2}} [-\tfrac{1}{4} (u/D)^3 + \tfrac{1}{8} (u/D)] \} \cos^2 \theta$$

$$- 2[1 - (u/D)^2]^{\frac{1}{2}} [-\tfrac{1}{3} (u/D)^2 + \tfrac{1}{3}] (u/D) \cos^2 \theta$$

$$+ \{ \tfrac{1}{8} \cos^{-1} (u/D) + [1 - (u/D)^2]^{\frac{1}{2}} [\tfrac{1}{12} (u/D)^3 - \tfrac{5}{24} (u/D)] \} \sin^2 \theta \Big) . \tag{20}$$

This can be rewritten as

$$K(\vec{u}, D) = \tfrac{1}{4} D^4 \Big(\tfrac{1}{8} \cos^{-1} (u/D) + [1 - (u/D)^2]^{\frac{1}{2}} \{ [\tfrac{1}{12} (u/D)^3 - \tfrac{5}{24} (u/D)]$$

$$+ [\tfrac{1}{3} (u/D)^3 - \tfrac{1}{3} (u/D)] [1 - (u/D)^2]^{\frac{1}{2}} \cos^2 \theta \} \Big) \tag{21}$$

If we now combine Eq.'s (13) and (21), we obtain

$$\langle (\alpha_1 - \alpha_2)^2 \rangle = \left(\frac{4}{\pi}\right)^4 \frac{\lambda^2}{D^4} \int d\vec{u} \left(\frac{1}{6} \cos^{-1}(u/D) + [1 - (u/D)^2]^{\frac{1}{2}} \{ [-\frac{1}{12} (u/D)^3 \right.$$

$$\left. - \frac{5}{24} (u/D)] + [\frac{1}{3}(u/D)^3 - \frac{1}{3}(u/D)] \cos^2 \theta \} \right) [\frac{1}{2}\mathcal{D}_\phi \ (\vec{S} + \vec{u})$$

$$+ \ \frac{1}{2}\mathcal{D}_\phi (\vec{S} - \vec{u}) - \mathcal{D}_\phi(\vec{u})] \qquad . \tag{22}$$

It will simplify our results if we now make the replacement

$$\vec{\mathcal{I}} = \vec{S}/D \qquad , \tag{23}$$

and after bringing in a factor of D^{-2} from outside the integral, make a change of variables, replacing u/D by u . This allows us to rewrite Eq. (22) as

$$\langle (\alpha_1 - \alpha_2)^2 \rangle = \left(\frac{4}{\pi}\right)^4 \left(\frac{\lambda}{D}\right)^2 \int d\vec{u} \ \{ \frac{1}{6} \cos^{-1}(u) + (1-u^2)^{\frac{1}{2}} \ [(\frac{1}{12} u^3 - \frac{5}{24} u) $$

$$+ (\frac{1}{3} u^3 - \frac{1}{3} u) \cos^2 \theta]\} \{\frac{1}{2}\mathcal{D}_\phi [D(\vec{\mathcal{I}} + \vec{u})]$$

$$+ \ \frac{1}{2}\mathcal{D}_\phi [D(\vec{\mathcal{I}} - \vec{u})] - \mathcal{D}_\phi (D\vec{u})\} \qquad . \tag{24}$$

At this point, we recall that we define θ as the angle between $\vec{u}$ and the x-axis. Operationally, the x-axis is defined by the fact that the component of angle-of-arrival that we are measuring lies in the x, z-plane. We will pick this component so that the x-axis makes an angle ψ with the aperture separation vector $\vec{S}$ (and with $\vec{\mathcal{I}}$) . This means that the angle between $\vec{u}$ and $\vec{\mathcal{I}}$ is $\theta + \psi$, so that we can write

$$|\vec{\mathcal{I}} \pm \vec{u}| = \{[\mathcal{I} \pm u \cos (\theta + \psi)]^2 + [u \sin (\theta + \psi)]^2\}^{\frac{1}{2}}$$

$$= [\mathcal{I}^2 \pm 2\mathcal{I}u \cos (\theta + \psi) + u^2]^{\frac{1}{2}} \qquad . \tag{25}$$

Taking note of the fact that the phase-structure function, $\mathcal{D}_\phi$, is dependent on only the magnitude of its argument, we see that we can rewrite Eq. (24) as

$$
\langle (\alpha_1 - \alpha_2)^2 \rangle = \left(\frac{4}{\pi}\right)^4 \left(\frac{\lambda}{D}\right)^2 \int\limits_0^{2\pi} d\theta \int\limits_0^1 u\, du \left\{ \tfrac{1}{8}\cos^{-1}(u) + (1-u^2)^{\frac{1}{2}} \left[\left(\tfrac{1}{12} u^3 - \tfrac{5}{24} u\right) \right. \right.
$$
$$
\left. + \left(\tfrac{1}{3} u^3 - \tfrac{1}{3} u\right) \cos^2 \theta \right] \right\} \left(\tfrac{1}{2}\mathcal{D}_\phi \left\{ D[\mathcal{J}^2 + 2\mathcal{J} u \cos (\theta + \psi) + u^2]^{\frac{1}{2}} \right\} \right.
$$
$$
\left. + \tfrac{1}{2}\mathcal{D}_\phi \left\{ D[\mathcal{J}^2 - 2\mathcal{J} u \cos (\theta + \psi) + u^2]^{\frac{1}{2}} \right\} - \mathcal{D}_\phi (Du) \right) \quad . \tag{26}
$$

Eq. (26) is the most general expression we can write for the mean-square angle-of-arrival difference. Its further evaluation can be carried out numerically as soon as we have an expression for the phase structure function, $\mathcal{D}_\phi$.

To proceed further in our evaluation, we introduce the approximation that the phase structure function can be accurately represented by the wave structure function. This allows us to write

$$
\mathcal{D}_\phi (x) \approx 6.88 \, (x/r_0)^{5/3} \quad , \tag{27}
$$

where r_0 is a length representative of the magnitude of the wavefront distortion. [3] If we use this approximation in Eq. (26), we obtain

$$
\langle (\alpha_1 - \alpha_2)^2 \rangle = 3.44 \left(\frac{4}{\pi}\right)^4 \left(\frac{\lambda}{D}\right)^{1/3} \left(\frac{\lambda}{r_0}\right)^{5/3} \int\limits_0^{2\pi} d\theta \int\limits_0^1 u\, du \left\{ \tfrac{1}{8} \cos^{-1}(u) \right.
$$
$$
+ (1-u^2)^{\frac{1}{2}} \left[\left(\tfrac{1}{12} u^3 - \tfrac{5}{24} u\right) + \left(\tfrac{1}{3} u^3 - \tfrac{1}{3} u\right) \cos^2 \theta \right] \right\}
$$
$$
\times \left\{ [\mathcal{J}^2 - 2\mathcal{J} u \cos (\theta + \psi) + u^2]^{5/6} + [\mathcal{J}^2 - 2\mathcal{J} u \cos (\theta + \psi) + u^2]^{5/6} - 2u^{5/3} \right\}
$$
$$
\tag{28}
$$

In this form our expression is directly suitable for computer evaluation. We take up the matter of this numerical evaluation and presentation of results in the next section.

- 55 -

Numerical Evaluation

To proceed beyond Eq. (28), it is convenient to introduce the quantity $I(\mathscr{S}, \psi)$, which we define by the equation

$$I(\mathscr{S}, \psi) = \left(\frac{16}{\pi}\right)^2 \int_0^{2\pi} d\theta \int_0^1 du\, u \left\{ \cos^{-1}(u) \right.$$
$$+ (1-u^2)^{\frac{1}{2}} \left[\left(\frac{1}{12} u^3 - \frac{5}{24} u\right) + (\tfrac{1}{3} u^3 - \tfrac{1}{3} u) \cos^2\theta \right] \right\}$$
$$\times \left\{ [\mathscr{S}^2 + 2\mathscr{S}u \cos(\theta+\psi) + u^2]^{5/6} + [\mathscr{S}^2 - 2\mathscr{S}u \cos(\theta+\psi) + u^2]^{5/6} - 2u^{5/3} \right\} \quad .$$

(29)

This allows us to rewrite Eq. (28) in the form

$$\langle (\alpha_1 - \alpha_2) \rangle = \frac{3.44}{\pi^2} \left(\frac{\lambda}{D}\right)^{1/3} \left(\frac{\lambda}{r_0}\right)^{5/3} I(\mathscr{S}, \psi) \quad . \tag{30}$$

This will serve as our final result, for all practical purposes. However, it is quite interesting to take note of the expression for mean square angle of arrival variation at a single aperture, $\langle \alpha^2 \rangle$, as given in Appendix B, Eq. (B-2), and recognize that we could rewrite Eq. (30) as

$$\langle (\alpha_1 - \alpha_2)^2 \rangle \approx \langle \alpha^2 \rangle I(\mathscr{S}, \psi) \quad . \tag{31}$$

Since α is a two-component tilt, i.e., it includes both x and y components in the mean square, while $\alpha_1 - \alpha_2$ represents the difference of two single component tilts, it would be necessary for α_1 and α_2 to be anti-correlated for $I(\mathscr{S}, \psi)$ to have a value greater than unity, and in no case could it be greater than two. In fact, we find it never gets to be quite as large as unity. The numerical evaluation of $I(\mathscr{S}, \psi)$ is a straightforward computer programming problem. We have prepared a program to carry out these calculations. The program is listed in Table III. 1, and the results for $I(\mathscr{S}, 0)$ and $I(\mathscr{S}, \tfrac{1}{2}\pi)$ are given in Table III. 2 for S= 1 to 20 in steps of $\tfrac{1}{2}$. As can be seen from

these results, for $\psi = 0$, I has values in the range of 0.5 to 0.75, approximately, while for $\psi = \frac{1}{2}\pi$, the values are somewhat smaller.

Discussion of Results

Our basic interest in all of this work has been in assessing the practicality of using mean square difference in angle of arrival measurements to determine the optical strength of turbulence along the propagation path, or more succinctly put, to determine r_0 . The critical question is how much larger $\langle (\alpha_1 - \alpha_2)^2 \rangle$ is expected to be than our measurement precision. From Eq. (30) and the fact that $I(\mathscr{J}, \psi)$ has a value of the order of 0.5 , we see that the mean square measurement value, which we call the signal squared, should be

$$(Sig)^2 \approx \frac{3.44}{\pi^2} \left(\frac{\lambda}{D}\right)^{1/3} \left(\frac{\lambda}{r_0}\right)^{5/3} \qquad . \qquad (32)$$

Our equipment will make measurements of single axis angle of arrival with some rms uncertainty, $\delta\theta$. The mean square variability in measurement of $\langle (\alpha_1 - \alpha_2)^2 \rangle$, which is our noise squared, is just the sum of the error for α_1 and for α_2 . Thus we can write for the noise,

$$(Noise)^2 \approx 2 (\delta\theta)^2 \qquad . \qquad (33)$$

The rms error in determination of r_0 , which we denote by δr_0 , can be determined from the equation

$$(Sig + Noise)^2 \approx \frac{3.44}{\pi^2} \left(\frac{\lambda}{D}\right)^{1/3} \left(\frac{\lambda}{r_0 + \delta r_0}\right)^{5/3} \qquad . \qquad (34)$$

Solving for δr_0 from Eq.'s (32), (33), and (34), using $\delta r_0 \ll r_0$, we get

$$\frac{\delta r_0}{r_0} \approx \frac{2.87 \ \delta\theta}{\left(\frac{\lambda}{D}\right)^{1/6} \left(\frac{\lambda}{r_0}\right)^{5/6}} \quad . \tag{35}$$

We see, for example, that if we work at $\lambda = 0.633$ μm , use aperture diameters of $D = 0.1$ m , and if $r_0 \approx 0.1$ m , (for which rms angle of arrival variation is $(3.44/\pi^2)^{1/2} (\lambda/D)^{1/6} (\lambda/r_0)^{5/6} = 3.74$ μrad), then we can achieve a measurement precision $\delta r_0 /r_0 \approx 4.53 \times 10^5 \ \delta\theta$. To get a 10% accuracy, the rms error $\delta\theta$ would have to be no greater than 0.22 μrad $\equiv 0.045$ arc seconds. If $\delta\theta \approx 0.1$ arc seconds, then $\delta r_0 /r_0$ would be of the order of 22%. If the propagation path were such that r_0 were 0.5 m (for which the rms angle of arrival variation is 6.66 μrad), then we would have $\delta r_0 /r_0 \approx 2.54 \times 10^5 \ \delta\theta$. To get a 10% accuracy, the rms error in $\delta\theta$ would have to be no greater than 0.39 μrad $\equiv 0.081$ arc seconds.

The feasibility of the experiment obviously depends critically on our ability to select propagation paths for which r_0 will be reasonably small, and on our ability to achieve a small enough value of $\delta\theta$.

If we can reliably obtain $\delta\theta \approx 0.1$ arc seconds, it should be possible to obtain useful measurement results. The basis for the data reduction of any such results is provided by Eq. (30), and the data in Table III.2.

References for Chapter III

1. D. L. Fried, "Statistics of a Geometric Representation of Wavefront Distortion," J. Opt. Soc. Am. 55, 1427 (1965).

2. H. B. Dwight, "Tables of Integrals and Other Mathematical Data," (The Macmillan Company, New York, 1957)

3. D. L. Fried, "Optical Heterodyne Detection of an Atmospherically Distorted Wave Front," Proc. IEEE 55, 57 (1967).

APPENDIX A of Chapter III

An alternate approach to the problem of treating angle-of-arrival statistics is to use the derivative of the phase function as a measure of the angle of arrival. Quite obviously, the derivative represents the wavefront tilt in a region of zero extent, and at least nominally there should be no difficulty in utilizing such an approach. We shall see, however, that this approach involves us in a divergence problem. With this formulation, the divergence is lifted by recourse to the inner scale of turbulence, providing smoothing over what otherwise would be a cusp in the statistics, i.e., $x^{5/3}$ has a cusp at $x = 0$. In an experiment, the smoothing would be provided by the finite size of the aperture diameter D, and results obtained using the derivative approach will depend on the inner scale of turbulence ℓ_0, where they ought to show dependence on D.

Using the derivative, we can write for the x-component of the local angle-of-arrival at $\vec{x}$,

$$\tilde{\alpha} = \left(\frac{\lambda}{2\pi}\right) \frac{\partial}{\partial x} \phi(\vec{x}) \quad , \tag{A-1}$$

so that the difference in x-components of the local angle-of-arrival at $\vec{x}_1$ and $\vec{x}_2$ can be written as

$$\tilde{\alpha}_1 - \tilde{\alpha}_2 = \left(\frac{\lambda}{2\pi}\right)\left[\frac{\partial}{\partial x_1} \phi(\vec{x}_1) - \frac{\partial}{\partial x_2} \phi(\vec{x}_2)\right] \quad . \tag{A-2}$$

The mean square difference can then be written as

$$\langle(\tilde{\alpha}_1 - \tilde{\alpha}_2)^2\rangle = \left(\frac{\lambda}{2\pi}\right)^2 \left\langle \left[\frac{\partial}{\partial x_1}\phi(\vec{x}_1) - \frac{\partial}{\partial x_2}\phi(\vec{x}_2)\right]\left[\frac{\partial}{\partial x_1'}\phi(\vec{x}_1')\right.\right.$$
$$\left.\left. - \frac{\partial}{\partial x_2'}\phi(\vec{x}_2')\right]_{\substack{\vec{x}_1'=\vec{x}_1 \\ \vec{x}_2'=\vec{x}_2}} \right\rangle \quad . \tag{A-3}$$

(This rather unusual notation introducing $\vec{x}_1'$ and $\vec{x}_2'$ is necessary so that when we carry out the multiplication and rearrange the terms, we can tell

which differentiation goes with which phase function.) Carrying out the multiplication, rearranging terms, and interchanging the order of ensemble averaging and differentiation, we obtain

$$\langle (\tilde{\alpha}_1 - \tilde{\alpha}_2)^2 \rangle = \left(\frac{\lambda}{2\pi}\right)^2 \left[\frac{\partial}{\partial x_1} \frac{\partial}{\partial x_1'} \langle \phi(\vec{x}_1) \phi(\vec{x}_1') \rangle - \frac{\partial}{\partial x_1} \frac{\partial}{\partial x_2'} \langle \phi(\vec{x}_1) \phi(\vec{x}_2') \rangle \right.$$

$$\left. - \frac{\partial}{\partial x_2} \frac{\partial}{\partial x_1'} \langle \phi(\vec{x}_2) \phi(\vec{x}_1') \rangle + \frac{\partial}{\partial x_2} \frac{\partial}{\partial x_2'} \langle \phi(\vec{x}_2) \phi(\vec{x}_2') \rangle \right]_{\substack{\vec{x}_1' = \vec{x}_1 \\ \vec{x}_2' = \vec{x}_2}} \quad (A-4)$$

The ensemble averages in Eq. (A-4) can be recognized as the phase covariance function. By adding-and-subtracting the phase variance, we can obtain the phase structure function, so that Eq. (A-4) can be rewritten as

$$\langle (\tilde{\alpha}_1 - \tilde{\alpha}_2)^2 \rangle = \left(\frac{\lambda}{2\pi}\right)^2 \left[-\frac{1}{2} \frac{\partial}{\partial x_1} \frac{\partial}{\partial x_1'} \mathcal{D}_\phi(\vec{x}_1 - \vec{x}_1') + \frac{1}{2} \frac{\partial}{\partial x_1} \frac{\partial}{\partial x_2} \mathcal{D}_\phi(\vec{x}_2' - \vec{x}_1) \right.$$

$$\left. + \frac{1}{2} \frac{\partial}{\partial x_2} \frac{\partial}{\partial x_1'} \mathcal{D}_\phi(\vec{x}_2 - \vec{x}_1') - \frac{1}{2} \frac{\partial}{\partial x_2} \frac{\partial}{\partial x_2'} \mathcal{D}_\phi(\vec{x}_2 - \vec{x}_2') \right]_{\substack{\vec{x}_1' = \vec{x}_1 \\ \vec{x}_2' = \vec{x}_2}} \quad . \quad (A-5)$$

We now note that if we introduce appropriate sum and difference coordinates, and hold the sum constant, then

$$\frac{\partial}{\partial x_i} \frac{\partial}{\partial x_j} \mathcal{D}_\phi(\vec{x}_i - \vec{x}_j) = - \frac{\partial^2}{\partial u_x^2} \mathcal{D}_\phi(\vec{u}) \quad , \quad (A-6)$$

where $\vec{u} = \vec{x}_i - \vec{x}_j$, and u_x denotes the x-component of $\vec{u}$. This means that we can rewrite Eq. (A-5) as

$$\langle (\tilde{\alpha}_1 - \tilde{\alpha}_2)^2 \rangle = - \left(\frac{\lambda}{x\pi}\right)^2 \left\{ \frac{\partial^2}{\partial S_x^2} \mathcal{D}_\phi(\vec{S}) - \left[\frac{\partial^2}{\partial S_x'^2} \mathcal{D}_\phi(\vec{S}')\right]_{\vec{S}' = 0} \right\} \quad , \quad (A-7)$$

where

$$\vec{S} = \vec{x}_2 - \vec{x}_1 \quad . \quad (A-8)$$

If we substitute the approximate form for the phase structure from Eq. (27) of the main text, the nature of our divergence problem becomes manifest. We obtain

$$\langle (\tilde{\alpha}_1 - \tilde{\alpha}_2)^2 \rangle = -\left(\frac{\lambda}{2\pi}\right)^2 6.88 \, r_0^{-5/3} \left\{ \frac{5}{3} \, (S_x^2 + S_y^2)^{-7/6} (\tfrac{2}{3} S_x^2 + S_y^2) \right.$$

$$\left. - \left[\frac{5}{3} \, (S_x'^2 + S_y'^2)^{-7/6} (\tfrac{2}{3} S_x'^2 + S_y'^2) \right]_{\substack{S_x' = 0 \\ S_y' = 0}} \right\} \, . \qquad (A-9)$$

The second group of terms in Eq. (A-9) is clearly divergent when $\vec{S}'$ is set equal to zero. We believe that the first group of terms accurately represents the $\vec{S}$-dependence of the mean square difference of the x-component of angle-of-arrival, but to get any use out of the result, we must find a way of renormalizing the divergence in Eq. (A-9). This renormalization can be provided by considering that Eq. (27) is only valid for values of x greater than or equal to the inner scale of turbulence ℓ_0. We argue that more properly the divergent term in Eq. (A-9) should be represented by the derivative evaluated at ℓ_0 rather than at zero. This then leads to a finite term of the order of $\ell_0^{-1/3}$ in place of the divergent term, and a result similar to our exact one obtained in the main text, but with the role of the aperture diameter D filled by the inner scale of turbulence, ℓ_0. Since for any practical experiment we will make D greater than ℓ_0, we conclude that the applicable renormalization would involve D rather than ℓ_0, with the accurate result being that obtained in the main text using Eq. (2) to obtain the tilt rather than the derivative procedure of Eq. (A-1) in this appendix.

APPENDIX B of Chapter III

It is necessary in the text to reference our mean square difference in angle-of-arrival results to the mean square angular variation for measurement on a single aperture. This calculation of the mean square angular variation has been carried out in reference 1, but without normalization. In this appendix, we shall use those results and only concern ourselves with the normalization.

If we let a_x and a_y denote the x and y components of tilt corresponding to a_{tilt} defined in Eq. (2), then from Eq. (7.8a) of reference 1[*], we have

$$\langle (a_x)^2 + (a_y)^2 \rangle = 0.883 \, (\tfrac{1}{4} \pi D^2) \, (D/r_0)^{5/3} \qquad . \tag{B-1}$$

As pointed out in the discussion just after Eq. (4) in the text of this report, a factor of $(\lambda/2\pi)(\pi D^4/64)^{-1/2}$ is required to convert the a_{tilt} coefficient to an angle-of-arrival coefficient α . Thus the mean square angle-of-arrival fluctuation for a single aperture of diameter D , summing the two components, should be

$$
\begin{aligned}
\langle \alpha^2 \rangle &= \langle (\alpha_x)^2 + (\alpha_y)^2 \rangle \\
&= \left(\frac{\lambda}{2\pi} \right)^2 \left(\frac{64}{\pi D^4} \right) \langle (a_x)^2 + (a_y)^2 \rangle \\
&= 1.027 \, \frac{3.44}{\pi^2} \left(\frac{\lambda}{D} \right)^{1/3} \left(\frac{\lambda}{r_0} \right)^{5/3} \qquad .
\end{aligned} \tag{B-2}
$$

---

[*] There is a factor of $\tfrac{1}{4} \pi D^2$ missing from the right-hand-side of Eq.'s (7.8a, b, and c) of reference 1. This can be traced back to a failure to pick up a factor of πR^2 in solving Eq. (4.4′) to obtain Eq.'s (4.6a, b, and c) in that paper.

Table III.1

Computer Program Listing

```
100 REM   **THIS PROGRAM CALCULATES THE NORMALIZED INTEGRAL
110 REM   **I(S,PSI) GIVEN IN EQ.(29), FOR THE MEAN
120 REM   **SQUARE DIFFERENCE IN ANGLE OF ARRIVAL AT TWO
130 REM   **POINTS SEPARATED BY THE NORMALIZED DISTANCE,
140 REM   **S .  PSI DENOTES THE ORIENTATION OF THE MEASURED
150 REM   **ANGLE OF ARRIVAL RELATIVE TO THE SEPARATION, S .
160 REM   **THE PROGRAM OUTPUTS ARE I(S) FOR PSI=0 DEG
170 REM   **AND J(S) FOR PSI=90 DEG.
200 DIM Z%,A$[35]
210 LET A$="##.#      +#.###↑↑↑   +#.###↑↑↑"
220 LET P=5/6
225 LET P2=5/3
230 LET PI=3.14159265
232 LET C=(16/PI)*(16/PI)*(2*PI/25)*(5E-20/3)
240 DEF   FNI(W)=(W*W+2*W*W*C+W*W)↑P+(W*W-2*W*W*C+W*W)↑P
250 DEF   FNJ(W)=(W*W+2*W*W*S1+W*W)↑P+(W*W-2*W*W*S1+W*W)↑P
260 DEF   FNA(W)=((W*W*W-2.5*W)/12+(W*W*W-W)*C*C/3)* COS (1-W*W)
270 DEF   FNC(W)= ATN ( SQR (1-W*W)/W)/2
280 FOR S=1 TO 20 STEP .5
290 LET I=0
300 LET J=0
310 FOR T=0 TO 24
320 LET T1=.251327*T
330 LET C= COS (T1)
340 LET S1= SIN (T1)
350 LET K=4
360 FOR W=5E-20 TO .95 STEP 5E-20
370 LET I2= FNC(W)
371 LET I2=I2+ FNA(W)
372 LET I2=I2*W
380 LET I1=I2*( FNI(C)-C*W↑P2)
390 LET J1=I2*( FNJ(C)-S↑↑P2)
400 LET I=I+W*I1
410 LET J=J+W*J1
420 IF W>2 GOTO 450
430 LET K=4
440 GOTO 460
450 LET K=0
460 PRINT W
470 PRINT T
480 LET I=C*I
490 LET J=C*J
500 PRINT USING A$;S;I;J
510 NEXT S
520 STOP
530 END
```

Table III.2
Calculated Values
for I(ℐ, ♦)

ℐ	I(ℐ, 0)	I(ℐ, ½π)
1.0	.+4.598E-01	+2.284E-01
1.5	+5.453E-01	+3.223E-01
2.0	+5.227E-01	+3.815E-01
2.5	+6.245E-01	+4.251E-01
3.0	+6.475E-01	+4.581E-01
3.5	+6.646E-01	+4.832E-01
4.0	+6.778E-01	+5.044E-01
4.5	+6.892E-01	+5.210E-01
5.0	+6.963E-01	+5.349E-01
5.5	+7.026E-01	+5.462E-01
6.0	+7.072E-01	+5.554E-01
6.5	+7.113E-01	+5.633E-01
7.0	+7.170E-01	+5.723E-01
7.5	+7.203E-01	+5.795E-01
8.0	+7.201E-01	+5.819E-01
8.5	+7.223E-01	+5.849E-01
9.0	+7.191E-01	+5.863E-01
9.5	+7.189E-01	+5.876E-01
10.0	+7.173E-01	+5.877E-01
10.5	+7.139E-01	+5.876E-01
11.0	+7.126E-01	+5.871E-01
11.5	+7.107E-01	+5.863E-01
12.0	+7.049E-01	+5.850E-01
12.5	+7.022E-01	+5.837E-01
13.0	+6.998E-01	+5.816E-01
13.5	+6.934E-01	+5.775E-01
14.0	+6.896E-01	+5.747E-01
14.5	+6.843E-01	+5.718E-01
15.0	+6.795E-01	+5.673E-01
15.5	+6.734E-01	+5.612E-01
16.0	+6.685E-01	+5.584E-01
16.5	+6.619E-01	+5.533E-01
17.0	+6.562E-01	+5.484E-01
17.5	+6.502E-01	+5.423E-01
18.0	+6.434E-01	+5.361E-01
18.5	+6.362E-01	+5.311E-01
19.0	+6.291E-01	+5.249E-01
19.5	+6.203E-01	+5.184E-01
20.0	+6.133E-01	+5.112E-01